

KPP-VOW Parameters flow velocities on dike slopes

Analysis of influence factors on wave run-up and overtopping flow velocities



KPP-VOW Parameters flow velocities on dike slopes

Analysis of influence factors on wave run-up and overtopping flow velocities

Author(s)

Nova Huppes

Vera van Bergeijk

KPP-VOW Parameters flow velocities on dike slopes

Analysis of influence factors on wave run-up and overtopping flow velocities

Client	Rijkswaterstaat Water, Verkeer en Leefomgeving
Contact	dr. ir. Myron. van Damme
Reference	-
Keywords	-

Document control

Version	1.0
Date	10-11-2022
Project nr.	11208034-001
Document ID	11208034-001-ZWS-0003
Pages	48
Classification	
Status	final

Author(s)

	Nova Huppes	
	Vera van Bergeijk	

Samenvatting

De snelheden van golfploop en -overslag worden beïnvloed door de geometrie en de ruwheid van de dijk. Een literatuurstudie is uitgevoerd naar de invloedsfactoren voor de oploopsnelheid en de snelheid van overslaande golven. In deze studie is gekeken naar de aannames van verschillende onderliggende studies om een beeld te krijgen hoe de invloedsfactoren in een probabilistische methode meegenomen kunnen worden en in de toekomst verbeterd kunnen worden. Dit onderzoek draagt bij aan het onderzoek naar een geharmoniseerde beschrijving van de snelheden die gebruikt worden in de beoordeling van de grasbekleding op het buitentalud (GEBU), kruin en binnentalud (GEKB).

De golfploophoogte wordt gebruikt om de oploopsnelheid te berekenen. De bekleding, de geometrie en de hoek van inval kunnen zorgen voor een afname in de oploophoogte. De invloedsfactoren die deze reductie beschrijven zijn veelal gebaseerd op onderzoek van 20 jaar geleden. Vanwege de beperkte hoeveelheid experimenten die toen zijn uitgevoerd is er voor de meeste invloedsfactoren niet genoeg data beschikbaar om deze factoren op een volledig stochastische manier mee te nemen. Naast het advies om kennis uit meer recente studies gerelateerd aan golfploopreductie te implementeren in de formules, is het belangrijk om nieuwe metingen voor golfploop uit te voeren om de formules uit te breiden en te verbeteren en om de nauwkeurigheid van gebruikte formules vast te kunnen stellen voor gebruik in een probabilistische methode.

De cumulatieve overbelasting methode (COM) bevat twee factoren voor snelheid van golfoverslag: de versnellingsfactor op het binnentalud en de belastingfactor voor overgangen en obstakels.

Hoewel een constante versnellingsfactor van 1.4 vaak gebruikt wordt vanwege praktische overwegingen, wordt de snelheid significant beïnvloed door de steilheid van het binnentalud en de initiële snelheid op de kruin. Daarom wordt vooralsnog het gebruik van de grafische methode voor de versnellingsfactor geadviseerd. Daarnaast zijn er analytische formules (Van Bergeijk et al., 2019; Van Gent 2002) beschikbaar voor een meer nauwkeurigere berekening van de snelheid langs de kruin en het binnentalud. Deze formules resulteren in een lagere snelheid aan het einde van de kruin en een grotere versnelling langs het binnentalud vergeleken met de grafische methode.

In een eerdere studie (Deltares, 2022d) zijn er verdelingen voor de belastingfactor voor verschillende overgangen afgeleid. Deze verdelingen komen overeen met recente studies naar overgangen, maar bevatten een grote onzekerheid in de belastingfactor.

Summary

Run-up flow velocities and overtopping flow velocities are influenced by the geometry and the roughness of the dike. A literature study on the influence factors for the flow velocities on the outer slope, the crest and the inner slope is performed to determine whether the influence factors can be included in a stochastic manner in failure probability computations. Moreover, the underlying assumptions provide insights in how the influence factors can be improved and extended in the future. This report is part of a larger research effort to find a harmonized expression for velocities that can be used to calculate the failure of the grass cover on the outer slope (GEBU), the crest and the inner slope (GEKB).

The run-up height is used to calculate the run-up velocity. The cover type, the geometry and the angle of wave attack can lead to a reduction in the run-up height. The influence factors describing this reduction are mostly based on research of 20 years ago. There is not enough data available for most influence factors to accurately include them in a stochastic manner due to a limited number of performed experiments. As a first step, the results of more recent studies to reduction in run-up heights can be implemented to improve the influence factors. However, studies of run-up heights and velocities are quite limited and therefore new measurements are necessary to significantly improve the formulas, extend the application range and to determine the accuracy of expressions used in a probabilistic method based on a mean-value approach.

The cumulative overload method (COM) includes two factors for the overtopping flow velocity on the crest and the inner slope: the acceleration factor on the inner slope and the load factor for transitions and obstacles. A constant acceleration factor of 1.4 is easy to use, but for now a graphical method is recommended since the flow velocity is significantly affected by the slope steepness and the initial flow velocity on the crest. Moreover, analytical formulas (Van Bergeijk et al., 2019; Van Gent 2002) are available for a more accurate calculation of the velocity along the crest and the inner slope. These formulas result in a decrease in velocity at the end of the crest and a higher acceleration along the slope compared to the graphical method. Distributions for the load factor for a number of transitions were derived in Deltares (2022d). These distributions agree with recent studies on transitions but do contain a large uncertainty in the load factor.

Contents

	Samenvatting	4
	Summary	5
1	Introduction	8
1.1	Overview of current projects concerning wave run-up and flow velocities	8
1.2	KPP-VOW Parameters flow velocities on dike slopes	9
2	Influence factors wave run-up	10
2.1	Introduction	10
2.2	Roughness (γ_r)	11
2.2.1	Smooth impermeable slopes	11
2.2.2	Placed block revetments	13
2.2.3	Armour rock	15
2.2.4	Roughness elements	16
2.2.5	Summarized roughness factors	16
2.2.6	Discussion	17
2.3	Oblique waves (γ_β)	18
2.3.1	Short-crested waves	18
2.3.2	Long-crested waves	19
2.3.3	Discussion	20
2.4	Composite slopes and berms (γ_b)	21
2.4.1	Discussion	24
2.5	Combinations of influence factors	24
2.6	Conclusions and discussion	25
3	The overtopping flow velocities	27
3.1	Introduction	27
3.2	The flow velocity along the crest and the landward slope	27
3.2.1	The acceleration factor in the COM	27
3.2.2	Formulas for the flow velocity on the crest	28
3.2.3	Formulas for the flow velocity on the landward slope	31
3.3	The effects of transitions and obstacles	32
3.3.1	Transitions in cover type	33
3.3.2	Slope changes	34
3.3.3	Obstacles	35
3.3.3.1	Height transitions	35
3.3.3.2	Objects perpendicular to the dike	36
3.3.3.3	Objects parallel to the dike	37
3.4	Discussion	37
4	Conclusions and recommendations	39
4.1	Conclusions	39

4.1.1	Conclusions – influence factors wave run-up	39
4.1.2	Conclusions – the overtopping flow velocities	39
4.2	Recommendations	40
4.2.1	Recommendations – influence factors wave run-up	40
4.2.2	Recommendations – the overtopping flow velocities	40
	References	42
A	Roughness factors TAW	46
B	Drag coefficients and shape parameters for objects	47

1 Introduction

1.1 Overview of current projects concerning wave run-up and flow velocities

The Netherlands contains hundreds of kilometers of dikes with a grass cover. This grass cover protects the dike against the loads caused by (overtopping) waves. It is important to be able to accurately assess the probability of failure of the grass cover, since this concerns the initial mechanism in the failure pathway where dike erosion eventually leads to a large flooding of the hinterland. Inaccurate failure probabilities of the grass cover can lead to either dikes that do not adhere to the legally required maximum probability of flooding or uneconomical dike designs.

Within BOI – the toolbox for safety assessment and design of flood defenses in The Netherlands – the failure of the grass cover is considered separately for the outer dike slope on the one hand, and the dike crest and inner slope on the other hand. These initial failure mechanisms are named GEBU (Gras Erosie BUITentalud / grass erosion outer slope) and GEKB (Gras Erosie Kruin en Binnentalud / grass erosion crest and inner slope), as indicated in Figure 1.1. Note that GEBU covers grass erosion due to both wave impacts and wave run-up. Only the latter is within the scope of this report, so in this report GEBU solely refers to grass erosion due to wave run-up.

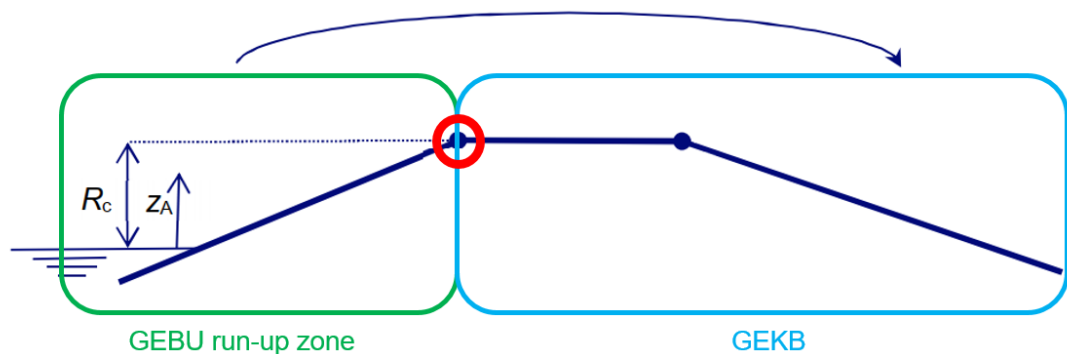


Figure 1.1 Schematic depiction of a dike and the domains of the GEBU run-up zone and GEKB initial failure mechanisms. The discontinuity in the existing velocity descriptions occurs on the outer crest line (red circle).

Both GEBU and GEKB include the Cumulative Overload Method (COM / Cumulatieve Overbelasting Methode) to calculate the failure of the grass revetment. In the COM, each wave run-up (GEBU) or overtopping (GEKB) event within the considered loading period of the dike is considered. The contribution to the total damage of each event is dependent on the flow velocity belonging to that event. Thus, when applying the COM it is important to relatively accurately predict the velocities of waves that run up the outer dike slope and (sometimes) overtop the dike crest and subsequently run down the inner dike slope.

Currently, GEBU and GEKB apply two different expressions to predict the flow velocity. These two expressions result in a discontinuity in the predicted flow velocity on the outer crest line of the dike. This is both physically unrealistic and impractical, and as such is mentioned as an issue in the 'Rode draad overstrooming door dijkerosie' (Deltares, RWS-WVL & HWBP, 2022). Research was initiated (Deltares, 2021a; Deltares, 2021b) to develop a harmonized expression for velocities that can be used both in GEBU and in GEKB. In 2022 this research is continued and is divided over three different projects. Deriving a new harmonized velocity expression is being done as a part of the KvK (Kennis voor Keringen / knowledge for flood defenses) project.

Within the KPP (Kennis Primaire Processen / knowledge primary processes) VOW (Versterking Onderzoek Waterveiligheid / strengthening flood safety research) project two subprojects on this subject are present. One is dedicated to identifying the influence of shallow water on run-up heights and velocities. The other is dedicated to evaluating the background of the different influence and acceleration factors (in)directly used within the COM method for GEBU and GEKB. These projects exchange knowledge extensively to maintain cohesion on this subject. It is foreseen that the knowledge developed within these projects, when mature enough, could be adopted and implemented by the BOI project in the near future. The (expected) deliverables of these projects are listed below.

- KvK 'stroomsnelheden grasbekleding' (11208057-037)
 - Report technical background harmonized velocity formula (Deltares, 2022a)
 - Report consequences of switch to harmonized expression (Deltares, 2022b)
- KPP-VOW 'parameters stroomsnelheden dijktaalud' (11208034-001)
 - Report technical background influence and acceleration factors (this report)
- KPP-VOW 'invloed waterdiepte op golfoverslag' (11208034-011)
 - Report data analysis of shallow water data for wave run-up (Deltares, 2022c)

1.2 KPP-VOW Parameters flow velocities on dike slopes

This report focusses on relevant parameters to describe flow velocities on dike slopes. Chapter 2 focusses on the run-up flow velocities (GEBU), and Chapter 3 describes the relevant parameters for overtopping flow velocities (GEKB).

Influence factors wave run-up height

Influence factors play an important role in run-up height predictions, which is why the origin of the factors is investigated in this literature study. The goal of this investigation is to understand the underlying assumptions of the different influence factors. This way it is possible to assess whether it is necessary to adapt them when switching from “a flood defence must be able to withstand once per X year loads” towards “the probability of flooding behind a flood defence should be less than Y% per year” (the change from the ‘probability of exceedance’ to the ‘probability of flooding’ philosophy, in which conservatism is unwanted).

Overtopping flow velocities

The overtopping flow velocity changes along the crest and the slope as the result of friction due to cover roughness and the gravitational acceleration along the slope. The changes in flow velocity from the start of the crest to other locations along the crest and slope is incorporated in the COM using influence factors that can also be applied to obstacles and transitions (which can also appear on the outer slope). Additionally, empirical and analytical models exist that describe the flow velocity on the crest and the inner slope. A comparison between the available methods to account for the changes in flow velocity along the crest and the inner slope is provided including the underlying assumptions to see whether and how the description of the flow velocity in the COM can be improved.

2 Influence factors wave run-up

2.1 Introduction

Formulas for wave run-up are derived for smooth impermeable and continuous slopes under perpendicular wave attack. Influence factors are used to consider the reduction of wave run-up due to the presence of circumstances that reduce the amount of run-up.

The currently prescribed method to predict run-up for dikes, are the equations given in TAW (2002). These are not the most recently available equations, but are prescribed by the Dutch law (Waterwet, Omgevingswet from 2023 onwards). More recent equations are given in EurOtop (2018). For this study, the equations from TAW (2002) are used as a starting point. Each section in this chapter starts with the equations from TAW (2002) and goes into the basis and possible weaknesses of the equations. In TAW (2002), the mean value of the wave run-up is expressed as:

$$\frac{R_{u2\%}}{H_{m0}} = 1.65 \cdot \gamma_b \cdot \gamma_f \cdot \gamma_\beta \cdot \xi_{m-1,0} \quad (1)$$

with a maximum of:

$$\frac{R_{u2\%}}{H_{m0}} = \gamma_f \cdot \gamma_\beta \left(4 - \frac{1.5}{\sqrt{\xi_{m-1,0}}} \right) \quad (2)$$

In general, the influence factors have a linear impact on the amount of run-up. In TAW (2002) and EurOtop (2007), hereafter EurOtop I, the berm factor is not present in the maximum run-up equation (Equation 2). In the equation for the maximum run-up (Equation 2), the berm factor is added next to the breaker parameter in EurOtop (2018, Equation 5.2), hereafter called EurOtop II. Due to the location of γ_b in EurOtop II, its impact on the maximum run-up is smaller than the other factors. Note that this reduced influence of a berm in EurOtop II is not based on (published) research.

This chapter gives an overview of the influence factors that are currently applied within BOI (EN: Safety Assessment and Design instruments, NL: Beoordelings- en Ontwerpinstrumentarium), which are the formulas of TAW (2002). For each influence factor the value or equation is given, after which the origin is investigated. Knowing the origin of the influence factors, it is possible to assess whether they are chosen conservatively or based on a mean value. Furthermore, it might be possible to see whether the factors are based on a Rayleigh distribution, and whether their effect on the front velocities or the maximum velocities are investigated in the original tests.

This study does not deal with the influence of seawalls, currents, and shallow foreshores. The report focusses on the influence factors that are most commonly applicable in combination with grass on the outer- or inner slope. The influence of water depth is not investigated in this study, since there is no influence factor on water depth used in TAW (2002). However, there is a dependency between run-up levels and water depth. This was researched by van Steeg et. al. (2020). The influence of water depth on run-up velocities is described in Deltares (2022c).

Virtually all available research into influence factors on wave run-up deal with the wave run-up height, and do not explicitly look into the influence on the run-up velocities. Hence the content of this chapter relates to wave run-up heights. The formulae for wave run-up velocities (or uprush) depend on the run-up height. Through this way, the influence factors on wave run-up height can be translated to velocities. However, due to the lack of systematic research into velocities, the validity of this approach cannot be verified.

2.2 Roughness (γ_f)

The roughness factor (γ_f) accounts for the run-up reduction due to the roughness of the revetment compared to a smooth slope. In this section, the roughness factors used in TAW (2002) are discussed, including their origin, to assess whether the factors are chosen conservatively or as a mean value based on a large range of tests.

In TAW (2002), a large table is given, which contains the roughness factors for the most common types of revetments used on Dutch dikes. This table is repeated in Appendix A, where the results from this study are added. These roughness factors are still used in EurOtop II to take the effect of revetments on the run-up reduction into account. The roughness factors from Appendix A are derived from several reference revetment types in the technical supplement to the TAW, TR23A (2002). The results of TR23A (2002) are based on run-up tests but are also being applied for overtopping.

2.2.1 Smooth impermeable slopes

Amongst others, smooth impermeable slopes are used in TR23A as a reference, for which the influence factor is set to 1. Figure 2.1 gives the results from these tests, which are executed in large scale facilities in Germany and The Netherlands.

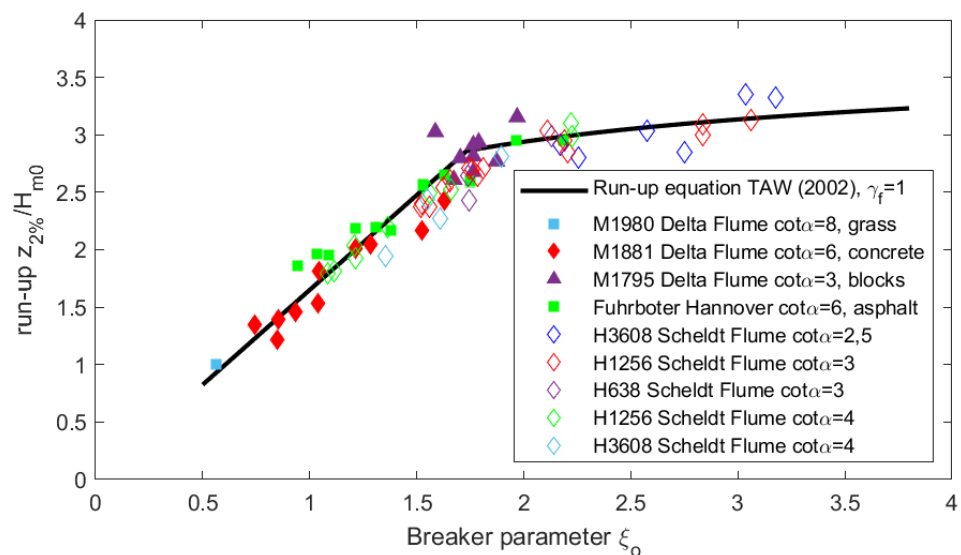


Figure 2.1 Results of run-up tests for smooth impermeable slopes from TAW (2002).

In Figure 2.1 the black line is the run-up equation as given in TAW (2002) for a roughness factor of 1. The markers give the results from different tests, for several types of revetments. Each type of revetment has a different marker, and is assessed in a different test series, the facility and slope angle of the revetment are depicted in the legend. The tests with 'blocks' (purple triangles) are performed with a layer of closed rectangular blocks. The data points below the black line have a roughness factor smaller than 1, the data points above the line give a roughness factor larger than 1 within the formula of TAW (black line). It could be counterintuitive to have roughness factors (or any influence factor) larger than 1. However, this is possible because the factors are derived from the TAW formula, which represents the average run-up height and has a standard deviation with possible results above and below this average. The standard deviation of the TAW formula leaves the possibility for the gamma values to have a mean value of 1 as well, with a standard deviation. For a smooth slope, with a (mean value) gamma of 1, this would lead to roughly half of the roughness factors being larger than 1.

On average, the different tests seem to have roughness factors varying around 1. This is also the conclusion within the TRA23A, therefore a roughness factor of 1 is used for these and similar revetments in TAW (2002). However, it should be noted that the conclusions are based on a small range of breaker parameter values. There are almost no results for high values of the breaker parameter. Furthermore, the number of tests on which the conclusions are based is very limited, especially for grass revetments (*i.e.* only one data point). In essence, the effective number of tests is limited for closed rectangular blocks as well, since the breaker parameter is around 1.8 for all tests.

In conclusion, the roughness factor for smooth impermeable slopes seems to be based on average values from large scale tests, but the amount of data is limited. The only available data point for grass is not within the breaker parameter range of the other types of revetments due to the very gentle slope (1:8). The TR23A does not mention the obtained run-up distribution or measurements of front velocities. Note that Equation 2 and the use of the roughness factor 1 for smooth impermeable slopes cannot be validated based on the mentioned large-scale tests.

The roughness factor of 1 for grass, given above, is assumed to be valid for significant wave heights larger than 0.75 m (TAW, 1997). For significant wave heights smaller than 0.75 m, the following equation to determine the roughness factor is suggested in TAW (1997) and adapted in EurOtop II to:

$$\gamma_f = 1.15H_{m0}^{0.5} \quad \text{for grass and } H_{m0} < 0.75m \quad (3)$$

A visual representation, along with the tests from Deltares (2014), is shown in Figure 2.2. The figure shows that three tests are performed for which the run-up level is determined. For all tests the found influence factor is lower than 1, even for the test where the significant wave height is larger than 0.75 m¹. Thus, the conclusion based on Figure 2.1 that the roughness factor for smooth impermeable slopes are based on average values from large scale tests, does not hold for grass covers.

¹ Note that in these tests, the wave run-up height on the grass slope was compared to that on a smooth concrete slope next to it, which enables the run-up of very thin water layers. It is not known what effect this has on the resulting influence factor, and its comparison to TAW (2002).

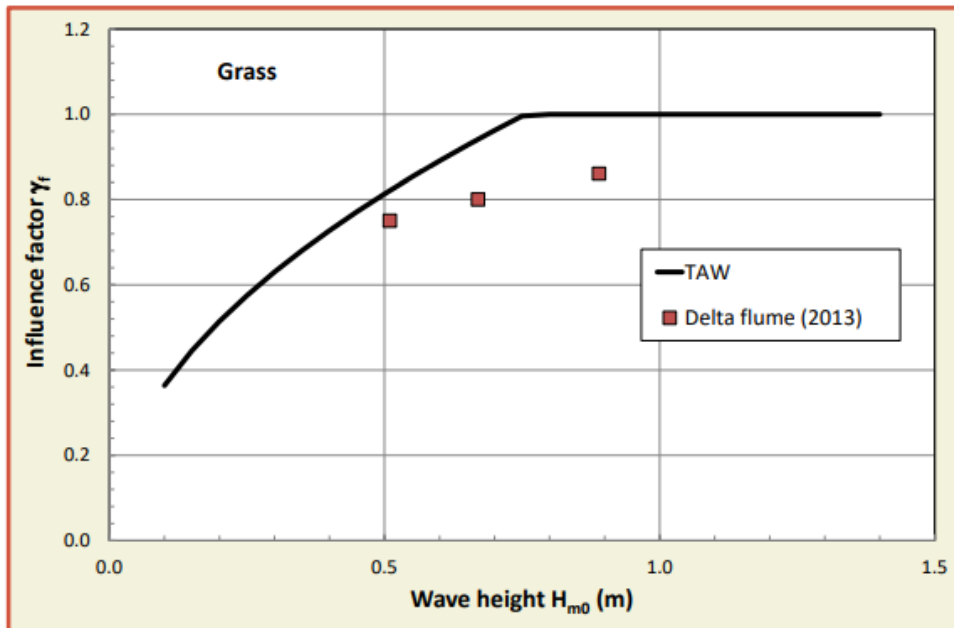


Figure 2.2 Influence factor for grass as presented in EurOtop (2018).

EurOtop II conservatively advises to use Equation (3) to determine the roughness factor for significant wave heights smaller than 0.75 m. Based on the Delta Flume experiments, the roughness factor could be lower, but this is based on a small number of tests. Deltares (2014) doesn't give an alternative equation based on the mean value of the tests. Based on the data shown in Figure 2.2 a mean value can be derived, but because of the small number of tests the uncertainty of such an equation would be large. Nevertheless, the number of data points is still larger than the single data point with a grass cover that was used to validate Eq. 1 for grass covers (Figure 2.1). To obtain more information on the uncertainties and biases of the equation, more tests are required.

2.2.2 Placed block revetments

In TR23A (2002), several run-up tests for placed block revetments are used to determine their roughness factors. These roughness factors are used as reference to derive the roughness factor of other revetments in TAW (2002) (see Appendix A). The results of the run-up tests are given in Figure 2.3, where also the predictions by wave run-up equations are shown (although these data points do not confirm the trends given by the expressions, the expressions predict levels of roughly similar magnitude). The tests are all executed in the former Delta Flume facility in Marknesse.

Note that the constant value of the influence factor is only valid in the linear part of the run-up formula. So, for values of ξ_0 up until 1.8, the value of γ_f is constant. For larger values of ξ_0 , the roughness factor increases linearly up to 1 for $\xi_0 = 10$. Which means that for the nonlinear part of the run-up formula, the roughness factor is described by:

$$\gamma_{f,surging} = \gamma_f + (\xi_0 - 1.8) \cdot \frac{1 - \gamma_f}{8.2} \quad (\text{eq. 6.1 in EurOtop II})$$

in EurOtop II, but the formula is already applied in TAW (2002).

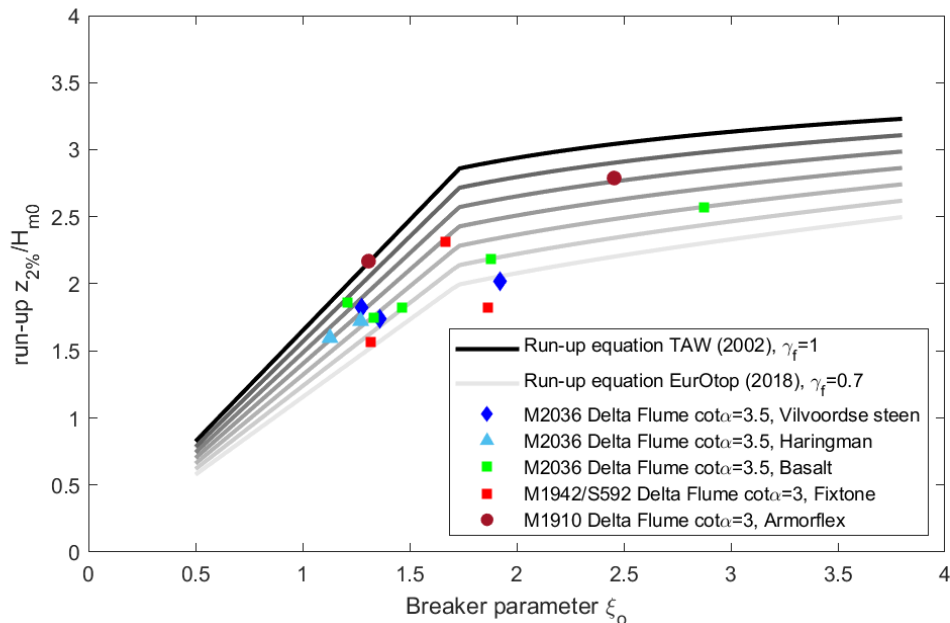


Figure 2.3 Results from run-up tests for placed block revetments from TR23A (2002).

TR23A shows that, in general, the influence of roughness is larger for larger breaker parameters, although the spread in the results is large. This would indicate that the roughness factor reduces for larger values of the breaker parameter, while the expression shows the opposite trend (*i.e.* higher values for the roughness factor for larger values of the breaker parameter). This indicates that the increase of the roughness factor towards 1 in the nonlinear part of the equation is a conservative approach.

For each of the tested placed block revetments, TR23A proposes a roughness factor. For each revetment, TR23A interpreted the results, reasoning for a certain value of the roughness factor:

- Vilvoordse steen: $\gamma_f = 0.85$. The number of tests is limited, containing a large spread in the results, so TR23A proposes to use the highest value for γ_f from the tests.
- Haringman: $\gamma_f = 0.9$. The results from the Haringman tests show only a small spread around a value of 0.85, but because there are only two tests available, a conservative value of 0.9 is chosen.
- Basalt: $\gamma_f = 0.9$. From the tests, roughness factors between 0.75 and 0.95 are found. TR23A makes a relatively conservative choice to use a roughness factor of 0.9 for basalt.
- Fixtone: $\gamma_f = 0.9$. Fixtone is a type of open asphalt. The results of the tests show a large variation in the obtained roughness factor. In TR23A, a factor of 0.9 is chosen, because Fixstone is rougher than asphalt, but a smaller roughness factor than 0.9 is not deemed desirable.
- Armorflex: $\gamma_f = 0.9$. The roughness factor from Armorflex is not chosen conservatively, but equal to basalt (0,9) because of comparable characteristics.

All the roughness factors for placed block revetments are in fact based on a very limited number of tests. For this reason, most of the roughness factors are based on conservative values. A first step to a probabilistic approach would be to use the average roughness factors obtained by the tests. However, because the number of tests is limited, a large deviation should be implemented as well. To obtain a better estimate of the roughness factors, more tests should be included in the data. Results for a broader spectrum of breaker parameters would give the best results, since the number of available results is especially low for large breaker parameters.

It is noted that the newest revetments have not obtained roughness factors in the most recent publications, such as EurOtop II. For instance, Quattroblock has been developed since, and didn't receive a roughness factor. For some new revetments, large scale tests have been executed in the former Delta Flume in Marknesse by Van Steeg et al. (2016). These tests determined the roughness factors of Hillblock, RONA®Taille and Verkaliit®GOR. These types of placed block revetments are categorized as channel shaped block revetments, due to the hollow sections around the blocks that absorb the up-rushing water, thereby dissipating some of the wave energy. Based on the average value from the tests, the roughness factor for channel shaped block revetments is defined as follows:

$$\gamma_{f,ru} = 0.0028 \cdot \frac{H_{m0}}{d_{channel}} + f \quad (4)$$

with $f = 0.69, 0.72,$ and 0.75 for respectively Hillblock, RONA®Taille, and Verkaliit® GOR. And $d_{channel}$ is the open volume of a placed block revetment per square metre.

2.2.3 Armour rock

Figure 2.4 gives the results of run-up tests for armour rock on an impermeable slope. The figure depicts the run-up equation used in TAW (2002) with a roughness factor of 1 and 0.55. The red markers represent run-up results from tests with single layered armour rock, the black markers are for tests with double layered armour rock. The results are interpreted by the TR23A as follows:

- Double layered armour rock: $\gamma_f = 0.55$. There are a lot of results available for double layered armour rock, covering a large range of breaker parameters. A factor of 0.55 is a fit based on the mean value of the available data according to TR23A.
- Single layered armour rock: $\gamma_f = 0.7$. There is less data available on single layered armour rock, although the roughness seems to be in line with the double layered armour rock. TR23A proposes a factor of 0.7 which is conservative since they suspected that scale effects played a role in the research.

Note that combinations of armour rock and grass further up the outer slope are not very common on dikes. For permeable slopes, relations are available in the Rock Manual, but are not deemed applicable on most dikes.

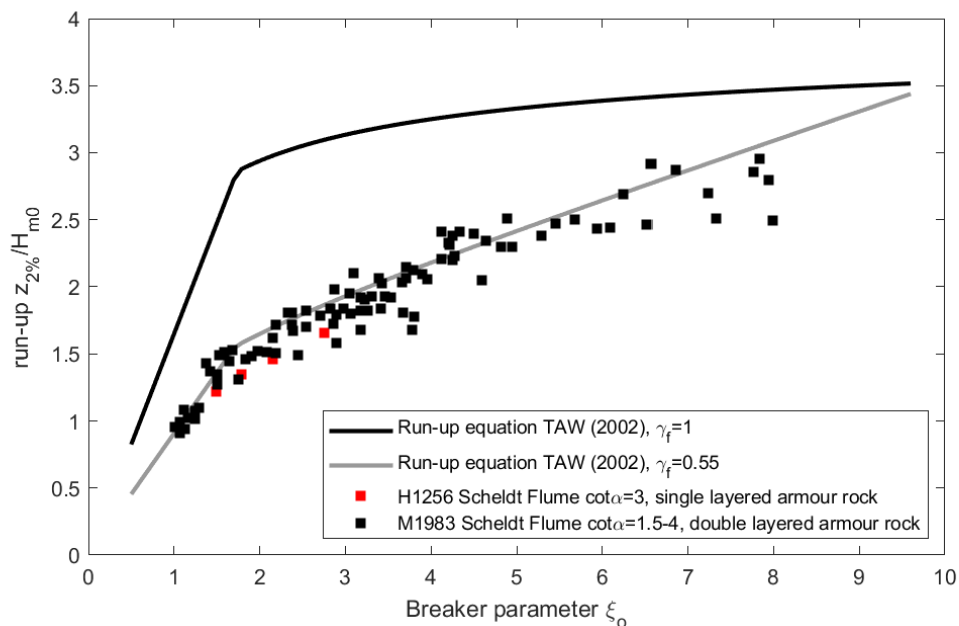


Figure 2.4 Results from run-up tests for armour rock from TR23A (2002)

The average value of 0.55 as a roughness factor for double layered armour rock seems appropriate. However, for larger breaker parameters the linear increase of the roughness factor towards 1 seems like a conservative choice. For the single layered armour rock, a roughness factor of 0.7 seems conservative as well. For a probabilistic approach, the average roughness factor should be used for single layered armour rock. Because the number of tests is limited, a large standard deviation should be implemented. Furthermore, one should investigate the possible scale effects that occurred during the tests. TR23A doesn't elaborate on the source of the scale effects, and further research found that the tests of double and single layered armour rock are executed in the same facility. Both test series are executed in the old Scheldt Flume in Marknesse, which at that time incorporated an (early version of) Active Reflection Compensation (ARC).

2.2.4 Roughness elements

Research towards roughness elements has started a long time ago, WL|Delft Hydraulics (1993) refers to research that is executed largely before 1960. More recently, the use of roughness elements was brought into practice for dikes by using placed block revetments with alternating heights, for instance in Breskens, Zierikzee and the new design of the Afsluitdijk. The most recent research towards roughness of protruding placed block revetments, are the works of Capel (2015), Chen et al. (2020) and Chen et al. (2022). All these recent studies use an average value approach to determine the roughness based on extensive testing, sometimes in combination with numerical studies.

2.2.5 Summarized roughness factors

Table 2.1 gives the roughness factors that are used as a reference to determine the roughness of other types of revetments. To determine the roughness of other revetments, comparison is made between photos from the reference revetments and other revetments. A complete overview of the roughness factors for all the revetments that are defined in TR23A (2002) is given in Appendix A. Some of the roughness factors in Appendix A are derived from an interpolation between two reference types. As described in the previous paragraphs, the roughness factors are mostly determined in TR23A (2002) and first used in TAW (2002). The factors are still applied in the latest EurOtop II publication.

Table 2.1 Roughness factors of reference type revetments as determined in TR23A (2002)

Reference type	Roughness factor γ_r	Comments
(smooth) concrete	1.0	Mean value, based on 10 tests in Delta Flume
Asphalt	1.0	Mean value, based on 11 tests in Hannover
Closed rectangular blocks	1.0	Mean value, based on 9 tests in Delta Flume with $\xi_0 \sim 1.8$
Grass ($H_{m0} > 0.75$ m)	1.0	Mean value, based on 1 test in Delta Flume
Grass ($H_{m0} < 0.75$ m)	$1.15H_{m0}^{0.5}$	Conservative equation
Vilvoordse steen	0.85	Highest value from 3 test results in Delta Flume (conservative)
Basalt	0.9	Conservative value within margin of 5 test results in Delta Flume
Haringman	0.9	Conservative value, higher than 2 test results from Delta Flume
Fixtone (open asphalt)	0.9	Conservative value, higher than 3 test results from Delta Flume
Armorflex	0.9	Factor based on roughness factor for basalt
Roughness elements	Depended on situation	Mean value
Double layered armour rock	0.55	Mean value, based on large number of tests in Scheldt Flume
Single layered armour rock	0.7	Conservative value, higher than 4 test results in Scheldt Flume

The research of Van Steeg et al. (2016) added roughness factors for channel shaped block revetments for Hillblock, RONA®Taille and Verkalit®GOR, based on an average value approach.

2.2.6 Discussion

The use of reference types to determine roughness of other revetments is debatable. The comparison is based on photos and expert judgement, and the criteria are quite unclear. However, investigating roughness factors by assessing each individual revetment by scale tests is costly. Here, the current translation from reference types to other revetments is applied due to lack of data. Note that, ideally, one would want to determine the roughness factor by executing the exact same tests both for a certain revetment type and for a completely smooth slope. The difference in results stems from the difference in roughness, since all other factors are kept constant. In practice this is not done to reduce costs. This means that the derivation of roughness factors directly depends on the empirical formula that is used to do so, while in theory this is not necessary.

For a mean value approach, which is necessary in probabilistic calculations, it is recommended to obtain more data from tests. This will give more insight in the uncertainties and biases of the currently used equations and influence factors. The only revetment type for which the roughness has been tested extensively is double layered armour rock. It is possible to obtain more data by adding measuring equipment to planned tests. More measurements require more time and effort but this way, more information is obtained from the same tests. With the information from these tests one can update the reference types and adjust the other revetments accordingly.

Recent model tests have shown that the roughness 'felt' by waves on a slope is dependent on the wave conditions and dike configuration. Chen et al. (2020) derived a new formulation for implementing roughness for dike overtopping. This formulation includes a relative freeboard, H_{m0} , breaker parameter and a coefficient dependent on the revetment type. A similar relation could be derived for the influence of roughness on wave run-up. Based on the present report, it is not possible to determine the best way to include roughness in the wave run-up. However, what can be concluded from the present report is that improvement is desirable. This starts

with additional data from run-up tests, and eventually proposing new values and/or formulations for the influence of roughness on run-up for dikes.

2.3 Oblique waves (γ_β)

The reduction factor for oblique waves (γ_β) accounts for the run-up reduction due to waves coming in under an angle, instead of perpendicular to the structure normal direction. In this paragraph, the equations for oblique waves used in TAW (2002) are discussed, including the origin, to assess whether the factor is defined conservatively or as a mean value based on a large range of tests.

2.3.1 Short-crested waves

In TAW (2002), the reduction factor for oblique short-crested waves is defined by:

$$\begin{aligned}\gamma_\beta &= 1 - 0.0022 |\beta| && \text{for } 0^\circ \leq \beta \leq 80^\circ \\ \gamma_\beta &= 1 - 0.0022 \cdot 80 && \text{for } |\beta| > 80^\circ\end{aligned}\tag{5}$$

In Hydra-NL and Riskeer, this factor was adopted differently. To ensure a smooth transition between angles of wave attack where run-up is occurring, and angles of wave attack where no run-up is expected any more ($>90^\circ$), the wave height and period are reduced for wave directions between 80° and 110° . This adaptation for Hydra-NL and Riskeer has not been included in the documentation of the software. The above equation is applied in the EurOtop II manual.

The equation originates from the report of WL|Delft Hydraulics (1993). Figure 2.5 gives the results of the tests on which the equation of WL|Delft Hydraulics (1993) is based. The tests are described in the report of Van der Meer and De Waal (1990). The tests are executed in the Vinjé facility 3D wave basin at the Marknesse location of WL. In this facility a model set-up is created of about 25 m long and wide. In the facility, waves were generated under an angle to create oblique incident waves. The model is placed under an angle to minimize wave reflection, however wall effects could have been present. For the study of Van der Meer and De Waal (1990), both long- and short-crested as well as regular and irregular waves are tested on the same model set-up. The same tests are performed on multiple geometries. The geometries consisted of a 1:2.5 slope, a 1:4 slope, and a 1:4 slope with a berm at the still waterline. The berm had a width of 5 times the significant wave height. For each geometry, tests are executed each with a different wave steepness. The s_{op} is varied between 1% and 5%.

The wave run-up height is measured with both a step gauge and by visual observation. The measurement points of step gauge had a mutual distance of 5 cm parallel to the slope, and a height above the slope of 3 to 4 mm. For the visual measurements, lines are made on the slope, so where model assistants could count how many times a wave reached a certain line. The different measurement methods are compared, and a constant offset of 3.2 cm along the slope is found between the measurement methods. The data of the step gauge is adjusted for the fact that wave tongues with a thickness smaller than 3 to 4 mm aren't measured. This explains the offset that is found between the measurement methods. Wave run-up velocities were not measured during the experiments.

For each geometry, first a test is executed with waves perpendicular to the structure. The run-up level found for this test is used as a reference for the other tests, so in the first test γ_β is 1. Van der Meer and De Waal (1990) assumed a Rayleigh-distribution of the run-up height, but also verified this assumption. They found some spread in the results but concluded that a Rayleigh-distribution is fitting for the highest run-up fractions.

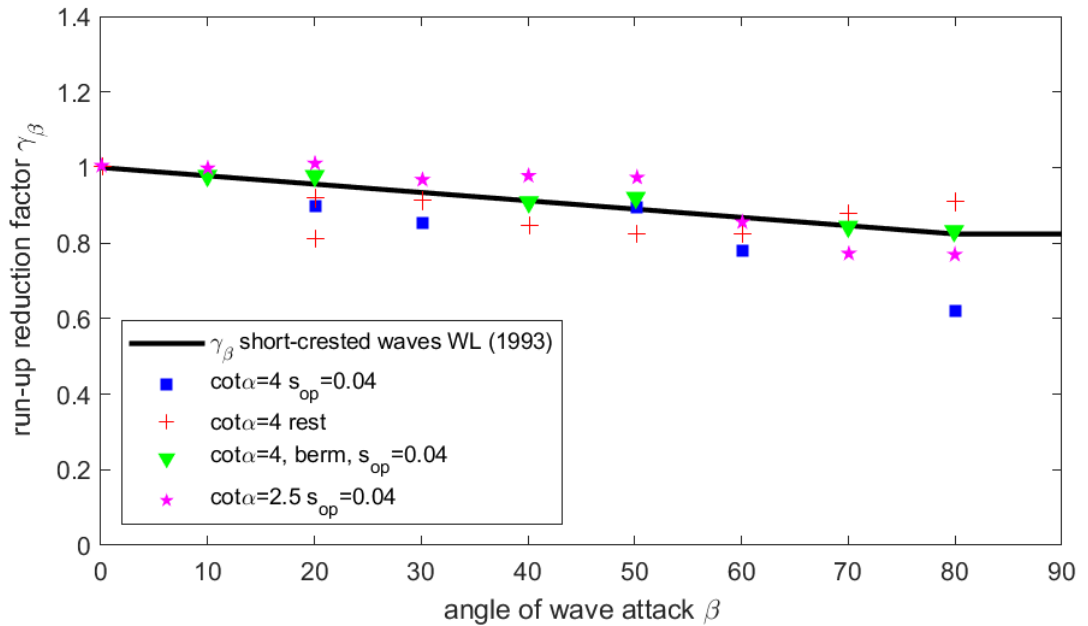


Figure 2.5 Results from run-up tests for oblique short-crested waves from WL|Delft Hydraulics (1993).

In the report of Van der Meer and De Waal (1990), equations for the reduction factor of both long- and short-crested waves are derived from the tests. However, these equations are derived to represent the upper limit of the reduction factors. The report by WL|Delft Hydraulics (1993) proposes Equation (5) to represent the average for the reduction of the wave run-up for short-crested, irregular waves. The equation is chosen because it is a simple formula that gives a good representation of the average value of the various tests. Because the natural variations in the results are not measured during the tests, it is also not possible to give a proper estimation of the spread in the results. The currently used equation seems to be a proper representation of the average run-up for the different angles of wave attack. For the biggest angles however, larger than about 50 degrees, the equation seems to be conservative, meaning that minimizing the influence factor is probably a conservative decision.

2.3.2 Long-crested waves

TAW (2002) doesn't provide a formula for wave run-up of long-crested waves. However, the report from WL|Delft Hydraulics (1993) on which the TAW (2002), and afterwards the EurOtop, run-up equations for short-crested waves are based, also provides an equation for long-crested waves:

$$\begin{aligned} \gamma_\beta &= \cos(|\beta| - 10^\circ) \text{ with a minimum of } \gamma_\beta = 0.6 \\ \gamma_\beta &= 1 \text{ for } |\beta| = 0^\circ - 10^\circ \end{aligned} \quad (6)$$

This equation, like the equation from the previous section, is intended to represent the average from the tests of Van der Meer and De Waal (1990). The executed run-up tests had the same model set-up as the above described tests for short-crested waves. The results of the tests are given in Figure 2.6. Like the results of the short-crested waves, the results for long-crested waves show large variations. For small angles of wave attack between 5 and 20 degrees, the equation seems to be conservative. For larger angles of wave attack, the variations in the results become smaller, and the equation seems a good fit to the average of the tests.

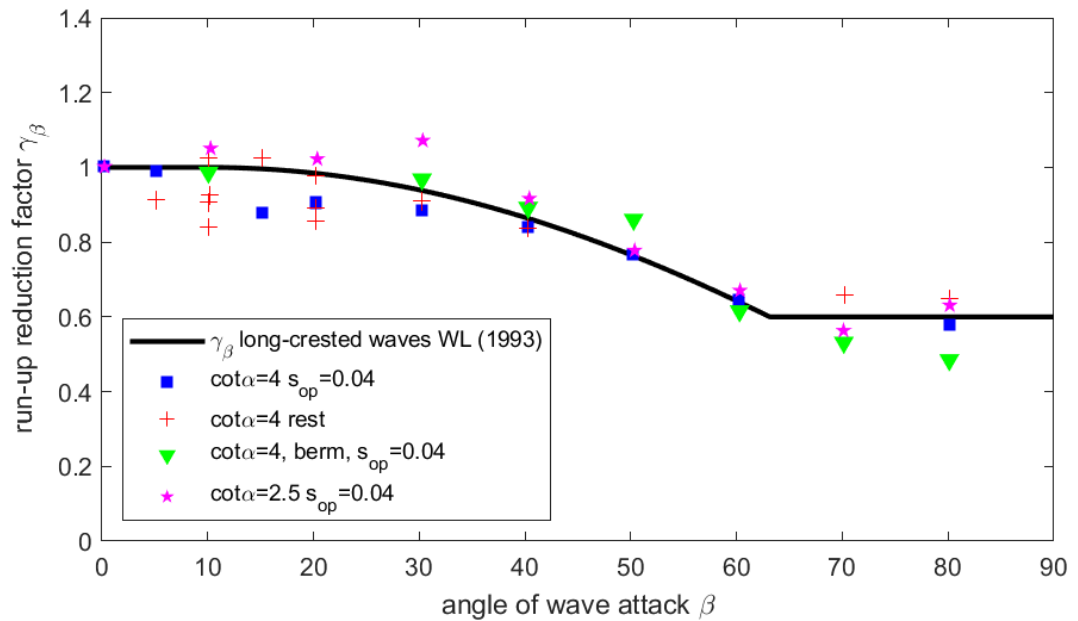


Figure 2.6 Results from run-up tests for oblique long-crested waves from WL|Delft Hydraulics (1993).

2.3.3 Discussion

The reduction factors for wave run-up that are derived for oblique wave attack aimed to describe the average of a series of model tests. For the most part, the equations represent the average value from several (small) scale wave run-up tests. The equation for short-crested waves is conservative for very large angles of wave attack ($\beta \geq 80^\circ$). The equation for long-crested waves is conservative for small wave angles ($\beta \leq 20^\circ$).

The tests included a geometry that incorporates a berm. In essence, the tests for this geometry combine the effects of oblique wave attack and the effect of berms. Because the test results of oblique wave incidence are compared to those with normally incident waves, it is still possible to isolate the effect of oblique wave incidence. However, by combining different influences (berms and oblique incidence), mechanisms could occur that are not overseen. For instance, for long-crested waves, the results of the geometry with a berm show a larger reduction than the other geometries. This is possibly caused by the fact that the relative berm width increases for oblique wave attack. For long-crested waves, this has been studied by Van Gent (2020). For short-crested waves, the results of the geometry with a berm agree with the geometries without berms.

The tests are performed on a relatively small scale. The tested water levels are between 0.36 and 0.72 m, and the wave heights between 0.06 and 0.12 m. However, because all tests are compared to a first test with perpendicular waves, scale effects are deemed relatively unimportant. A possibly larger inaccuracy caused by the Vinjé facility, is that no state-of-the-art wave generation and ARC was present and the size of the wave basin was relatively small. This means that during the tests, waves were reflected within the facility. The sides of the facility had wave dampening structures and the structure was placed under an angle to prevent reflection as much as possible, but some reflection could not be prevented.

Van Gent & Van der Werf (2019) studied wave overtopping on steep permeable slopes in the case of oblique wave attack. Physical model tests are performed in the Delta Basin facility at Deltares. It was found that for the tested structure the difference between long- and short-crested waves is negligible for the influence of oblique waves on overtopping. This differs from the conclusions in WL|Delft Hydraulics (1993) regarding impermeable structures. Van Gent &

Van der Werf (2019) derived a single formula for both short- and long-crested waves that fits the latest data better than the equations from TAW (2002). Especially for short-crested waves, large deviations are found between the test results and the TAW (2002) expressions. Based on tests with long-crested oblique waves Van Gent (2020) poses that it is likely that also for short-crested waves on (impermeable) dikes with and without a berm, an alternative formulation also outperforms the influence factor from WL|Delft Hydraulics (1993). The Delta Basin facility that is used to obtain the data is 50 metres long and wide (four times larger than the Vinjé facility) and includes an ARC system. Since the new facility is much larger than the facility in Marknesse, an extra advantage is that the influence of lateral boundaries will be smaller in general. Since the equations for overtopping in TAW are derived in a similar way to the run-up equations, the expectation is that the run-up equations will exhibit large deviations as well when new model tests are executed. It is recommended to perform a similar study for the influence of oblique waves on wave run-up.

2.4 Composite slopes and berms (γ_b)

The reduction factor for berms (γ_b) accounts for the run-up reduction due to presence of berms or different slope angles within the geometry of the structure. In this section, the influence factor for berms, used in TAW (2002) is discussed, including the origin, to assess whether the factor is defined conservatively or as a mean value based on a large range of tests.

In TAW (2002), the berm influence for both run-up and overtopping is defined by:

$$\gamma_b = 1 - r_B(1 - r_{db}) \quad \text{for } 0.6 \leq \gamma_b \leq 1.0$$

With:

$$r_B = \frac{B}{L_{Berm}}$$

And:

$$r_{db} = 0.5 - 0.5 \cos\left(\pi \frac{d_b}{R_{u2\%}}\right) \quad \text{for a berm above still water line}$$

$$r_{db} = 0.5 - 0.5 \cos\left(\pi \frac{d_b}{2 \cdot H_{m0}}\right) \quad \text{for a berm below still water line}$$

$$r_{db} = 1 \quad \text{for berms lying outside the area of influence}$$

where r_B represents the influence of the berm width, and r_{db} the influence of the height of the berm. B is the horizontal width of the berm and L_{berm} is the width of the berm plus the horizontal distance to the locations $1 \cdot H_{m0}$ below and above the berm. d_b is the level of the berm above still water level. The above equation is applied in the EurOtop II manual, of which the visualisation of the parameters above are shown in the figure below.

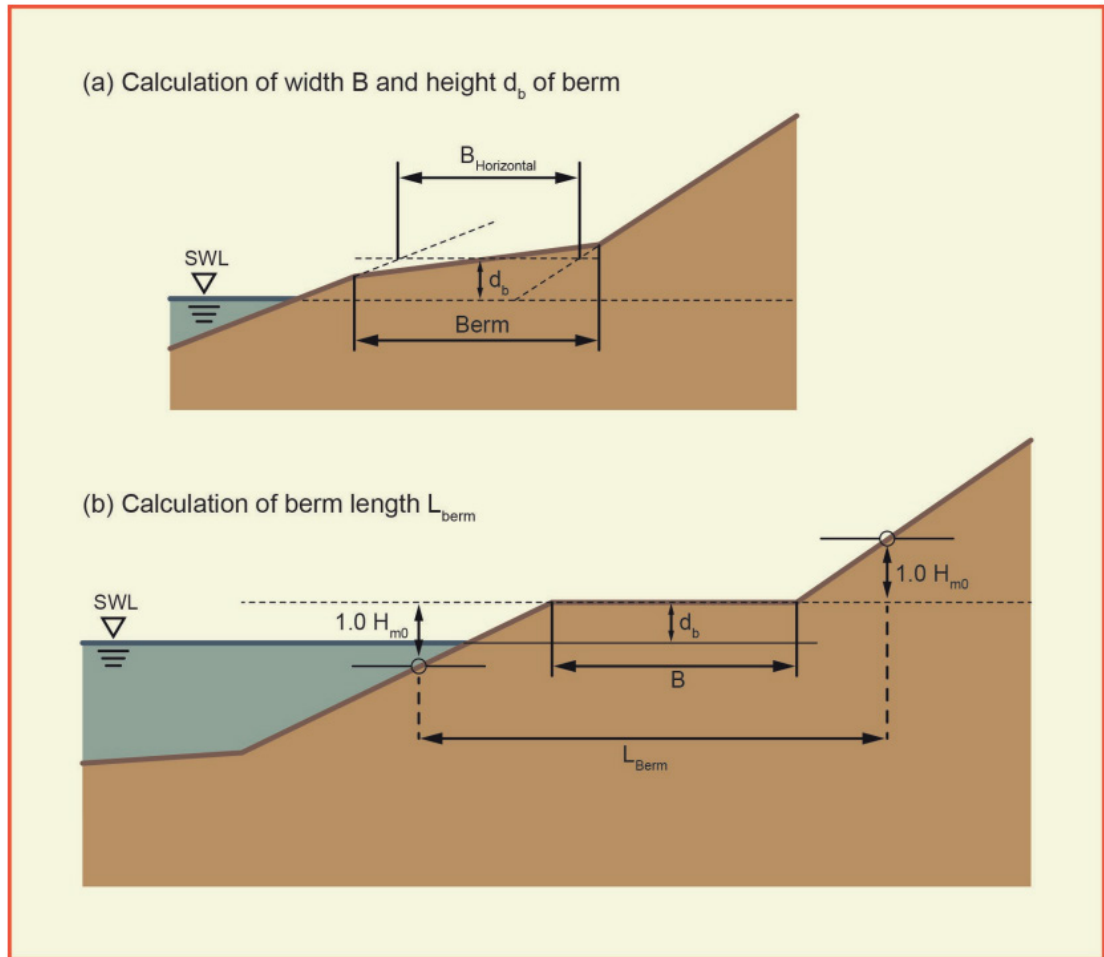


Figure 2.7 Definitions of parameters relevant for berms as presented in EurOtop (2018).

The equation used in TAW (2002) deviates from the proposed equation by WL|Delft Hydraulics (1993). The expressions for r_B and r_{db} differ between the two reports. In WL|Delft Hydraulics (1993), the parameter r_B is originally proposed as the ratio between the slope angle of the structure with a berm, and without a berm. In TAW (2002) this parameter is rewritten to the above ratio between B and L_{berm} . This is described in WL|Delft Hydraulics (1997). In essence, this parameter remains unchanged, but the way of representing the parameter is different.

What also changed between WL|Delft Hydraulics (1993) and TAW (2002), apart from parameter r_B , is the parameter r_{db} . In WL|Delft Hydraulics (1993), this parameter is defined as:

$$r_{db} = 0.5 \cdot \left(\frac{d_b}{H_{m0}} \right)^2 \quad \text{with } 0 \leq r_{db} \leq 1 \quad (8)$$

where d_b is again the level of the berm above still water level and H_{m0} is the significant wave height. For berms below the still water line (SWL), it is possible to make a comparison between the equation for r_{db} from WL|Delft Hydraulics (1993) and TAW (2002). The result is shown in Figure 2.8, which gives the value of r_{db} for berm heights between SWL and $2 \cdot H_{m0}$ below SWL. When the value of r_{db} goes towards 1, the berm factor γ_b also becomes 1. A smaller value of r_{db} also results in a small berm factor. Looking at Figure 2.8, this means that for berm depths from 0 to H_{m0} below the SWL, the different equations give more or less the same results. From about H_{m0} below SWL and lower, the equation of WL|Delft Hydraulics (1993) leads to higher values for the run-up level.

For berms above the SWL, it is not as straight forward to make a comparison between the two equations for r_{db} . This is because in the new equation, r_{db} iteratively depends on the run-up level on the dike ($R_{u2\%}$). This means that the value of r_{db} is, amongst others, dependent on the wave period and the other influence factors, such as the roughness. Because of these extra dependences, it is suspected that the value of r_{db} in the TAW (2002) will differ significantly from the original equation in WL|Delft Hydraulics (1993).

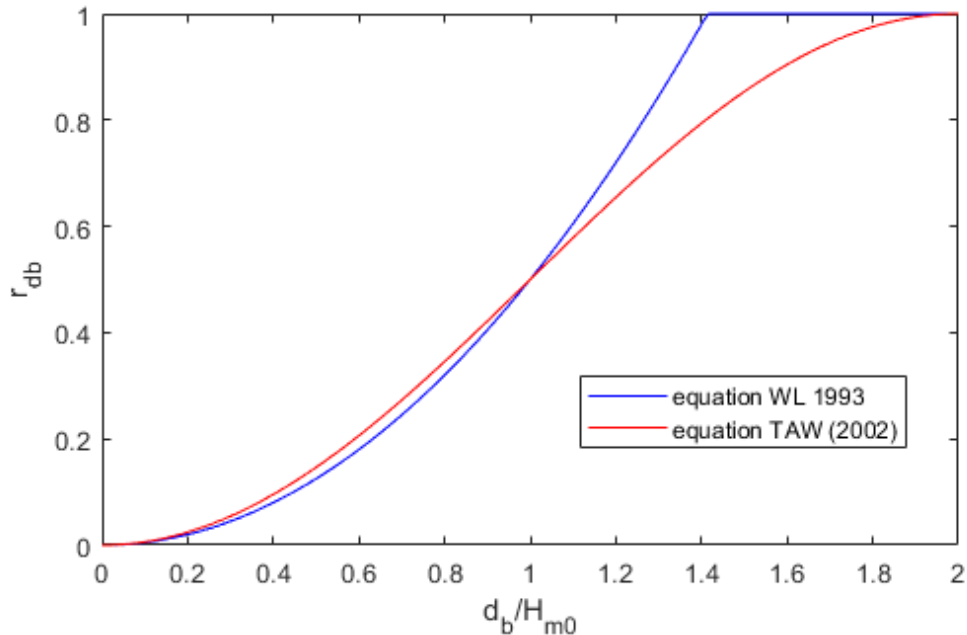


Figure 2.8 Factor r_{db} according to the equation of WL|Delft Hydraulics (1993) and TAW (2002)

In the tests described by WL|Delft Hydraulics (1993), several geometries and boundary conditions are tested. The influence of a berm at the still waterline is tested for two different equivalent slope angles. One of 1:3 and one with an equivalent slope angle of 1:4. For both equivalent slope angles, the depth of the berm in relation to the SWL is varied. Berms with a height of 1 and 1.5 H_{m0} above and below the SWL are tested. Also, three different berm widths are tested. For all tests, the slope angle of the berm is 1:15. The tests are executed in the Scheldt Flume in Marknesse, which contained an ARC installation in its wave generator. During the experiments, the run-up height is measured by a counter, therefore not the timeseries and velocities. Although the executed tests showed a large spread in the results, the equations as proposed in WL|Delft Hydraulics (1993) are set to represent an average.

The formula from the TAW (2002), which is used in EurOtop II, is derived from a different interpretation of the tests described in WL|Delft Hydraulics (1993). In general, smooth transitions are strived within the run-up formulations. Especially when working towards a probabilistic approach, it is undesirable to have unexpected transitions in the outcome of the equations. This led to the decision to change the factor r_{db} to the smoother equation used in TAW (2002) and thereafter. For berms above the water level, the decision towards the dependence on $R_{u2\%}$ in the formula stemmed from the fact that the berm influence in the new equations is zero for berms on a level of $R_{u2\%}$, again contributing to smooth transitions. The formulations of WL and TAW (2002) are similar for the most important area, berms around the water level. The cosine function is similar to the quadratic function for berms around the water level, but represents the physics better, being the importance of the $R_{u2\%}$ for berms above the water level. Because of the large spread in the original results, it is possible that the new equations are a good fit to the data as well. However, this does not seem to be studied.

2.4.1 Discussion

The influence factor that accounts for the presence of berms is equal for overtopping and run-up. Although these mechanisms are different, research on overtopping could be insightful for run-up. Recent research on the influence of berms on overtopping includes the work of Van Gent (2020), Chen et al. (2020) and Chen et al. (2022). This research involved both physical and numerical investigations to assess the influence of berms, but also roughness and oblique wave attack on wave overtopping at dikes.

Chen et al. (2020) found that the influence of berms on the amount of overtopping depends on the wave steepness. They proposed a new equation for γ_b , which is similar to the equation that is currently used in TAW (2002) and EurOtop II, but incorporates a factor $c_b/\sqrt{s_{m-1,0}}$:

$$\gamma_b = 1 - c_b \frac{r_B(1 - r_{db})}{\sqrt{s_{m-1,0}}} \quad \text{with } 0.6 \leq \gamma_b \leq 1.0 \quad (9)$$

The incorporation of $s_{m-1,0}$ makes the influence factor directly dependent on the wave steepness. Note that for berms above the SWL this is already indirectly incorporated through the dependence of r_{db} on $R_{u2\%}$. In the above equation, c_b is a coefficient which in Chen et al. (2020) is calibrated for several situations. It is found that c_b is 0.21 for an impermeable berm and 0.13 for a permeable berm covered by open blocks.

According to Van Gent (2020) the equations for r_B and r_{db} are not validated extensively in the derivation of Equations (7) and (9). This means that the expressions for r_B and r_{db} may not be optimal, which again influences the values found for coefficient c_b . Although Equation 9 appears to account for the influence of berms more accurately than the method applied in BOI (TAW, 2002), it is better to revisit the influence factor for berms on wave run-up before implementing new formulations for γ_b that have been derived for wave overtopping. Based on the research of Chen et al. (2020) it was found that for overtopping, the berm influence increases as the wave steepness decreases. If the same holds for wave run-up, the currently used influence factor could be conservative for some, and non-conservative for other conditions.

2.5 Combinations of influence factors

In TAW (2002), influence factors are considered separately. The separate factors are multiplied as shown in Equations (1) and (2). Interaction of different run-up reduction factors is not considered. It is possible that the different mechanisms influence each other, which is currently not considered in TAW (2002). Little research is available on this subject. The executed experiments for oblique wave attack from Section 2.3 contained tests with oblique wave attack for a construction with a berm. However, only the relative run-up reduction is considered, the run-up for oblique wave attack is compared to the run-up for perpendicular wave attack (both including a berm). This means no conclusions can be given about the combined effect of oblique wave attack on a construction with a berm. Similarities between wave run-up and wave overtopping processes indicate however, that the combination of influence factors without taking potential combined influences into account (e.g. combinations of roughness and berms, or combinations of berms and oblique waves), may introduce inaccuracies (see Chen et al, 2020, 2022 and Van Gent (2020)). Applying TAW (2002) for the combination of a berm and oblique waves is likely to lead to conservative results, based on physical reasoning and assuming some similarity between effects on wave run-up and on wave overtopping.

It is unknown if more research has been conducted on the influence of combinations of influence factors on wave run-up. Van Gent (2020) studied the influence of a combination of oblique wave attack and berm influence on overtopping using experimental research in the Delta Basin at Deltares. The following relation was found for the influence of oblique wave attack on geometries with a berm:

$$\gamma_{\beta} = \cos^2 \beta + 0.35 \cdot (1 - \cos^2 \beta) \left(1 + \frac{B}{H_{m0}}\right)^{-1} \quad (10)$$

Some additional testing is required to validate the equation to broaden the area of validity, especially for wave run-up instead of wave overtopping, but the equation is a first step towards combining influence factors for berms and oblique waves. Using a similar approach, the combined influence of oblique waves and berms, or other combinations of influence factors, on run-up could be tested.

2.6 Conclusions and discussion

In general, influence factors for wave run-up applied in existing manuals stem from research done more than 20 years ago. This research was generally executed using a JONSWAP spectrum at the toe of dikes, which means that free incoming infra-gravity waves (waves generated by wave breaking on the foreshore) are not taken into account. Furthermore, virtually all available research into influence factors on wave run-up deal with the wave run-up height, and do not explicitly look into the influence on the run-up velocities. In the current BOI practice, the influence on the run-up height is taken into account, which is then used as input for the formula to calculate run-up velocities. Due to the lack of systematic research into velocities, however, the validity of this approach cannot be verified.

Recently, research has been done on roughness factors for new types of revetments, but the relations derived in 1993 (for oblique waves) and in 2002 (roughness and berms) are still used in EurOtop II. Since then, much advancement has been made in the equipment of experimental facilities and the approach for the assessment and design of dikes in the Netherlands. At the time when the influence factors were derived, Dutch dikes were mostly designed according to a conservative and deterministic approach. Today, a probabilistic approach is used for dike design and failure. To obtain an appropriately accurate probability of flooding, it is important to have a proper average value and possibly even a probability distribution for each influence factor. At this point, it is unknown if it is possible to implement stochastic influence factors in BOI. Ideally, all relevant parameters in BOI are stochastic, since this will lead to the best probabilistic prediction of dike failure and design. However, too many stochastic values may lead to unworkable computational times. Furthermore, improper implementation of stochastic values could lead to influence factors unjustly becoming the leading parameters in calculations. This could for instance occur when the probability distribution of a parameter is very wide because there are few experiments available or when the spread in the results is very large. This should be considered when deriving stochastic distributions for influence factors. At this point, for most influence factors, not enough data is available to fully implement a stochastic approach. Nevertheless, ignoring the uncertainty in the influence factors also has consequences and is not in line with the current approach within BOI.

Recent studies mostly focus on wave overtopping, not on wave run-up. In the studies where wave run-up is measured, run-up velocities are often not measured. This is likely because wave run-up is harder to measure than overtopping, and run-up velocities are even more difficult. This makes the data less or unsuitable to investigate run-up velocities for a better prediction of grass cover erosion. Through the $R_{u2\%}$ it is possible to estimate the run-up velocity, although this is less accurate than measuring the run-up velocities directly. For grass covers run-up, and specifically run-up velocities are important for its strength. Many Dutch dikes have grass covers on the (upper part of its) outer slope and on the inner slope, making a good estimation of run-up velocities essential.

Considering the different influence factors that have been considered in this chapter, it can be concluded that an average value approach is attempted when deriving the influence factors.

However, when limited data is available, conservative decisions are made. This is mostly the case for various roughness factors. For oblique waves, the equations for the influence of both long- and short-crested waves is based on an average from several tests. However, these tests are performed in 1990, in a facility that didn't contain wave generation and active wave absorption techniques that are now state-of-the-art. As described in Section 2.3.3, new tests for the influence of oblique waves on overtopping have shown that the equation that is proposed in TAW (2002) and EurOtop II isn't very accurate for overtopping. This is probably no different for wave run-up.

It is recommended to first examine the available studies on run-up reduction that have been executed since the derivation of the currently used reduction factors (from TAW, 2002). However, recent tests mainly focus on wave overtopping, so the amount of available data on wave run-up is likely very limited. After all available data has been examined, new experimental research on influence factors on wave run-up is needed. Tests for the influence of oblique waves is deemed to be a logical first step that requires the least number of tests to derive an improved formula. New experiments fulfil both the purpose of validating some older data (for instance the tests from the Vinjé facility), as giving a better basis to base the influence factors on average values. In the present probabilistic method to evaluate dikes, conservative choices are only made when very little data is available. For the influence of oblique short-crested waves on wave run-up, the TAW (2002) provides conservative estimates. For the combination of oblique wave and a berm, TAW (2002) is likely to provide conservative estimates as well. The scarce data on wave run-up at dikes with grass covers indicate that using TAW (2002) is likely to be conservative as well. To account for the influence of berms on wave run-up levels, it is likely that the method by TAW (2002) is conservative for some wave conditions, and non-conservative for other wave conditions. It is recommended to revisit the influence factors for wave run-up at dikes (with grass covers), since applying influence factors by TAW (2002) for a mean-value approach as proposed in BOI, leads to an unknown accuracy of the outcome of the evaluation of dikes.

3 The overtopping flow velocities

3.1 Introduction

Once the wave run-up height exceeds the crest height, the waves flow over the crest and flow down along the landward slope. The change in flow velocity along the crest and the landward slope depends on the geometry including the cover type, the crest length, the slope length and the slope steepness. Transitions and obstacles also affect the overtopping flow velocity (Deltares, 2013; Van Bergeijk, 2022a).

In the COM, the damage number D is calculated by summing over the flow velocity of each overtopping wave U_i that is larger than the critical velocity U_c .

$$D = \sum_{i=1}^N \alpha_m (\alpha_a U_i)^2 - \alpha_s U_c^2 \quad \text{for } \alpha_a U_i > U_c. \quad (11)$$

where N is the number of overtopping waves. Influence factors are used in the version of the COM that is currently applied within BOI: the acceleration factor α_a accounts for the acceleration along the landward slope, the load factor α_m accounts for the increase in load due to transitions and obstacles and the strength factor α_s accounts for a reduction in strength near transitions and obstacles. These influence factors are locally applied and do not affect the flow velocity downstream of obstacles and transitions. Next to these influence factors, empirical and analytical formulas are available to calculate the flow velocity on the crest and the landward slope. This chapter provides a comparison of the influence factors in the COM and the available empirical and analytical formulas in literature. The assumptions of both the influence factors and the formulas are discussed as well as their applicability range.

3.2 The flow velocity along the crest and the landward slope

3.2.1 The acceleration factor in the COM

In the cumulative overload method, the acceleration factor α_a describes the variation in front velocity along the crest and the landward slope. In general, the front velocity will decrease on the crest ($\alpha_a < 1$) and increase on the landward slope ($\alpha_a > 1$). The graphical method in Figure 3.1 is available to determine the acceleration factor based on the slope steepness, the slope length and the flow velocity on the crest U_0 (Deltares, 2015). In Deltares (2015) the increase in flow velocity is calculated for a grass cover using the formulas of Schüttrumpf (2005), see also Table 3.2 discussed in Section 3.2.3. The main limitation of the graphical method is that the effect of the overtopping volume on the acceleration is not taken into account and the acceleration factor is not available for other slope steepness's, cover types and flow velocities.

For practical reasons, in Deltares (2019, 2022d) a constant acceleration factor of 1.0 for the crest and 1.4 for the landward slope is used to determine the influence of transitions and objects. In general, the large overtopping volumes lead to damage of the grass cover and these volumes have an acceleration of approximately 1.4 for slopes between 1:2.3 and 1:4 (Deltares, 2017). Using a constant acceleration factor means that the effect of slope length, slope steepness, cover roughness and overtopping volume on the flow velocity is not considered. This generally leads to an overestimation of flow velocity of the smaller overtopping volumes, however, these smaller overtopping volumes have no or a limited contribution to the damage and erosion of the grass cover (Deltares, 2022d). For longer slopes applying a constant factor 1.4 leads to a systematic underestimation of the velocities.

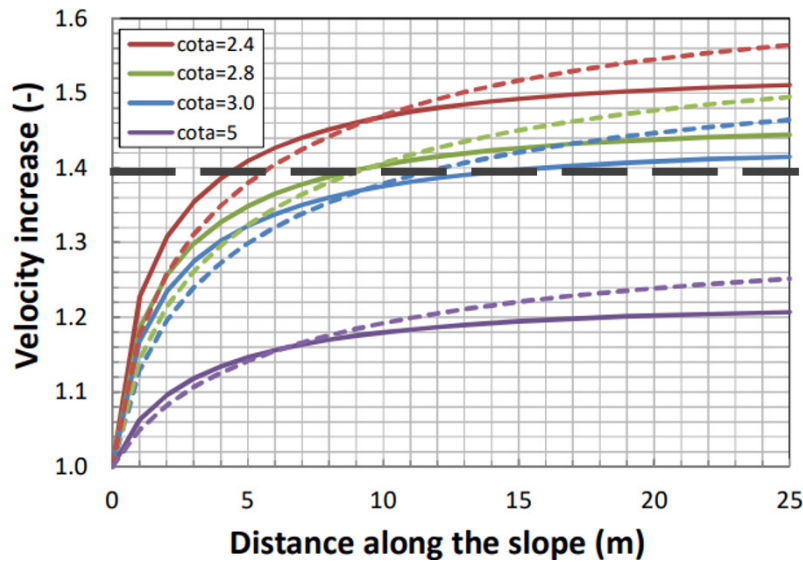


Figure 3.1 The velocity increase of overtopping wave volumes over the landward slope. Solid line: $U_0 = 4$ m/s, dashed line: $U_0 = 6$ m/s. The black dashed line indicates the constant acceleration factor of 1.4.

3.2.2 Formulas for the flow velocity on the crest

The flow velocity and the layer thickness on the start of the crest ($x_c = 0$) is determined by the run-up height $R_{u2\%}$ and the crest freeboard R_c . These flow parameters are the initial conditions for the overtopping flow on the dike crest (EurOtop, 2018). Physical model tests (Schüttrumpf, 2001; Van Gent, 2022) have been performed to develop empirical formulas for the 2% exceedance layer thickness $h_{2\%}$ and flow velocity $u_{2\%}$ at the start of the crest ($x_c = 0$)

$$h_{2\%}(x_c = 0) = c_{A,h} (R_{u2\%} - R_c) \quad (12)$$

$$u_{2\%}(x_c = 0) = c_{A,u} (g(R_{u2\%} - R_c))^{0.5} \quad (13)$$

The empirical coefficients $c_{A,h}$ and $c_{A,u}$ vary between multiple studies (Table 3.1) due to different dike configurations as well as differences in the experimental instruments and the methods to determine the 2% exceedance values. Some studies assumed that the coefficients depend on the slope angle of the seaward slope α (Bosman, 2007; Van der Meer et al, 2010). Additionally, the studies of Van Gent (2002) and Chen et al. (2022) include the roughness influence factor γ_f in Equations (12) and (13) to account for the reduction in friction when the calculated run-up height is higher compared to the crest level.

A new formula for the flow velocity ($U_{i\%}$) is developed in Deltares (2022a) to improve the calculation of both the run-up flow velocity on the seaward slope and the flow velocity at the start of the crest. This formula can be used in the future as initial condition to calculate the flow velocity along the crest and the landward slope.

Table 3.1 The coefficient for the layer thickness $C_{A,h}$ and flow velocity $C_{A,u}$ on the seaward crest line with the slope angle of the seaward slope α .

Source	$C_{A,h}$	$C_{A,u}$	Slope steepness
Schüttrumpf (2001)	0.33	1.37	1:3, 1:4, 1:6
Van Gent (2002)	0.15	1.33	1:4
Bosman (2007)	$0.010/\sin^2(\alpha)$	$0.30/\sin(\alpha)$	1:4, 1:6
Van der Meer et al. (2010)	0.13	$0.35 \cot(\alpha)$	1:3, 1:4, 1:6
EurOtop (2018)	0.2 for slopes 1:3 and 1:4 0.25 for slopes 1:5 0.3 for slopes 1:6	1.4 - 1.5	1:3 - 1:5
Formentin et al. (2019)	$0.085 \cot(\alpha)$	$0.12 \cot(\alpha) + 0.41$	1:2, 1:4

Table 3.2 Formulas for the flow velocity on the crest u_c and the landward slope u_s as function of the cross-dike coordinate x . The flow velocity depends on the layer thickness h , the crest width B_c , the friction factor f , the time t , the landward slope angle φ , the wave length L_0 and the momentary discharge Q .

Study	Crest	Landward slope
S2001 Schüttrumpf (2001)	$\frac{h_c(x_c)}{h_c(x_c = 0)} = \exp(-0.75x_c / B_c)$ $\frac{u_c(x_c)}{u_c(x_c = 0)} = \exp\left(-\frac{fx_c}{2h_c(x_c)}\right)$	$u_s(x_s) = \frac{u_{s,0} + \frac{k_1 h_s}{f} \tanh\left(\frac{k_1 t}{2}\right)}{1 + \frac{f u_{s,0}}{h_s k_1} \tanh\left(\frac{k_1 t}{2}\right)}$ $t \approx -\frac{u_{s,0}}{g \sin \varphi} + \sqrt{\frac{u_s^2}{g^2 \sin^2 \varphi} + \frac{2x_s}{g}}$ $k_1 = \sqrt{\frac{2fg \sin \varphi}{h_s}}, h_s = \frac{u_{s,0} \cdot h_{s,0}}{u_s}$
EurOtop (2018)	$\frac{u_{2\%}(x_c)}{u_{2\%}(x_c = 0)} = \exp(-1.4x_c / L_0)$	Same as Schüttrumpf (2001)
VB2019 Van Bergeijk et al. (2019)	$u_c(x_c) = \left(\frac{fx_c}{2Q} + \frac{1}{u_c(x_c = 0)}\right)^{-1}$ $Q = u_c(x_c = 0) \cdot h_c(x_c = 0)$	Same as Van Gent (2002): $u_s(x_s) = \frac{\alpha}{\beta} + \mu \exp(-3\alpha\beta^2 x_s / \cos \varphi)$ $\alpha = \sqrt[3]{g \sin \varphi}, \beta = \sqrt[3]{f / 2Q},$ $\mu = u_s(x_s = 0) - \frac{\alpha}{\beta}$

On the crest, the flow velocity decreases due to friction and depends on the roughness of the cover and crest width B_c . The formula in the EurOtop II manual is an empirical formula to describe the decrease in the 2% exceedance flow velocity. This formula does not include the effect of cover roughness and might not be accurate for crests with roughness.

Schüttrumpf (2001) and Van Bergeijk et al (2019) derived analytical formulas for the flow velocity on the crest (Table 3.2). The roughness of the cover is described in both analytical formulas using the friction factor f that is calibrated to 0.01 for grass covers (SBW, 2012). In both cases, the flow velocity depends on the layer thickness on the crest. Schüttrumpf (2001) derived an empirical formula for the decrease in the layer thickness on the crest. Van Bergeijk et al (2019) uses continuity of discharge to calculate the layer thickness and thereby it is assumed that all the water flows towards the landward slope. For low velocities this assumption might not be valid for the seaward edge of the crest.

The S2001 formulas are derived from the 2D continuity equation and momentum equations based on experiments in a small (100 m x 2 m x 1.25 m) and large wave flume (300 m x 5 m x 7 m). The formulas are only validated for a smooth cover with a friction factor of 0.058. The formulations are derived using a no slip boundary conditions, a horizontal crest and the local acceleration (du/dt) is neglected compared to convective acceleration ($u du/dx$).

The VB2019 formulas are derived from the 1D shallow water equations and are validated for both flume and field tests with varying cover types. The main assumption is that diffusion of the wave is much smaller compared to advection, which holds for most cases except combinations of small overtopping volumes and very rough covers. The formula for the crest is also applicable to other horizontal parts of the dike, such as a horizontal berm on the landward slope, and can calculate the overtopping flow velocity over horizontal parts with transitions in cover type (Van Bergeijk, 2022a).

Van Bergeijk et al (2019) determined the performance of the three formulas for the flow velocity on the crest for both flume and field tests. The results showed that the EurOtop (2018) formula overestimated the flow velocity for the flume tests, but the formula performs well for the field tests on grass-covered crests. The S2001 formula underestimated the flow velocity for both the field data and the flume data. Both the VB2019 formula and the EurOtop (2018) formula perform well on the crest, but the EurOtop (2018) formula cannot be applied to non-smooth since the formula does not include a roughness coefficient.

Only a limited number of measurements for the flow velocity on the crest are available. For the majority of the wave overtopping tests, the flow velocity is only measured at either the start or the end of the crest and therefore information on the change in flow velocity on the crest is limited to those edges. Physical model tests mainly focus on the amount of wave overtopping and the flow velocity at the seaward crest line, and therefore these tests do not provide information on the flow velocity along the dike crest. The same test results as obtained by Van Gent (2002) have been used by Van Bergeijk et al (2019) to calculate the decrease in flow velocity over the crest for flume tests with a scale model of wood and rough stones. In addition, Van Bergeijk et al (2019) used measurements of the flow velocity on the crest over a distance of 2 m during a test with the wave overtopping simulator on a grass-covered dike (Van Hoven, 2013). This data shows that the flow velocity decreases on the crest for all the measurements with a grass cover and wood, while the flow velocity remains constant (≈ 1) for a rough stone cover (Figure 3.2). The VB2019 formula underestimates the decrease in flow velocity compared to the measurements for the grass cover. However, the measurements for the grass cover are uncertain since the first measurement location is close to the outlet of the simulator. The flow at this location could be influenced by the simulator and therefore not representative for the overtopping flow in reality. Measurements of the flow on the dike crest generated with the wave run-up simulator are more reliable since the flow has more time to develop, but these measurements are not available.

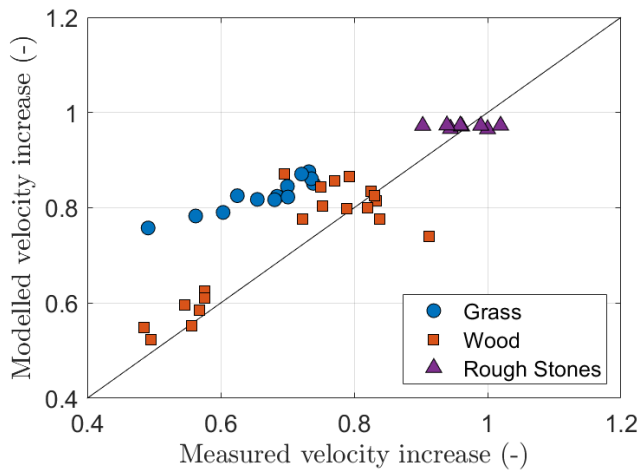


Figure 3.2 The decrease in flow velocity on the crest determined from the measurements of Van Gent (2002) for a wood and rough stone cover and the experiment at Millingen (Deltares, 2013) for a grass cover compared to the velocity decrease calculated with the VB2019 formula for the crest.

3.2.3 Formulas for the flow velocity on the landward slope

The acceleration of the overtopping flow along the landward slope depends on

- the cover type
- the flow velocity at the end of the crest
- the overtopping volume
- the dike geometry described by the length of the slope and the steepness of the slope

Two analytical formulas are available to calculate the flow velocity along the landward slope (Table 3.2). The S2001 formula needs to be solved in an iterative manner and is therefore time consuming (Deltares, 2013). This is one of the practical reasons why a constant acceleration factor is used in Deltares (2019, 2022d). However, the analytical formulas of Van Gent (2002) (see also Van Bergeijk et al., 2019) do not need to be solved in an iterative manner and are therefore computationally faster and more practical.

The analytical formulas describe the acceleration of the wave due to gravitational acceleration until a balance with the bed friction is achieved. Deceleration of the wave along the landward slope is not described by these formulas. Deceleration occurs due to spreading of the wave as the result of bed friction and thereby reducing both the layer thickness and flow velocity at the front. Both formulas assume continuity of discharge at the wave front ($u \cdot h = \text{constant}$) which is a valid approximation for overtopping flow (Hughes, 2011).

The S2001 formulas are validated with physical model tests with smooth structures ($f = 0.058$) and landward slopes of 1:2 to 1:6. The S2001 formulas are further validated for grass-covered slopes in Deltares (2013) using measurements of the flow velocity during field tests with the wave overtopping simulator resulting in a calibrated friction factor of 0.01 for grass. The S2001 formula is time-dependent and needs to be solved in an iterative manner for both time and space. Additionally, the effect of changes in cover type or geometry on the flow velocity cannot be calculated using the S2001 formula because these changes can lead to instabilities.

The VB2019 formula is based on the derivation in Van Gent (2002) and is validated using both flume data with varying cover roughness and dike geometries as well as field data of the wave overtopping simulator experiments on grass-covered dikes. In the study of Van Bergeijk et al (2019), the performance of the VB2019 formula is compared to the S2001 formula indicating that the VB2019 formula performs better compared to the S2001 formula for all tests, since the S2001 formula underestimates the flow velocity for both the flume and field tests.

Figure 3.3 shows a comparison of the calculated flow velocity increase from the crest to the landward toe using the analytical formulas S2001 and Van Gent (2002) (see also VB2019) for all overtopping waves during a storm. The storm is characterised using an average overtopping discharge q and a significant wave height H_s to generate distribution of overtopping volumes during the storm that are translated to flow velocities on the crest using an empirical formula in Van der Meer et al. (2010). The VB2019 formula predicts a higher increase in flow velocity compared to the S2005 formula. The constant acceleration factor of 1.4 underestimates the increase in flow velocity for the majority of the overtopping waves, except for some of the larger overtopping volumes.

The main implication is that the constant acceleration factor underestimates the acceleration for all waves except the largest. The underestimation of the acceleration can partly be explained by the S2001 formula that underestimate the acceleration and are the basis for the acceleration factor. Additionally, the acceleration factor is based on the acceleration of the larger wave volumes since these are the main cause of the cover damage. However, Figure 3.3 shows that a constant acceleration factor underestimates the acceleration of all overtopping waves during a storm with $H_s = 1$ m and $q = 10$ l/s/m, which can lead to a significant underestimation of the load during this storm. On the other hand, the COM is calibrated using the acceleration factor and this underestimation of the load is balance by the calibrated values for the critical velocity and the thresholds for the damage number.

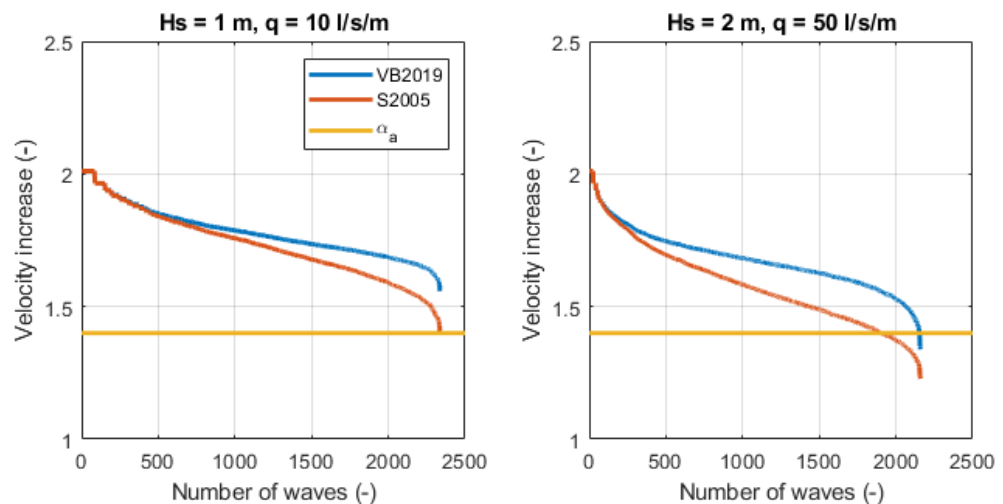


Figure 3.3 Comparison of a constant acceleration factor α_a , the iterative method of S2001 and the analytical approach of Van Gent (2002) and VB2019 for the overtopping waves characterised by the significant wave height H_s and the average overtopping discharge q for a landward slope of 1:3 with a length of 15 m.

3.3 The effects of transitions and obstacles

The load factor α_m in the COM describes the increase in load due to transitions and obstacles. The COM only includes a load based on the flow velocity, while other processes such as turbulence and impact forces can also result in high loads on the cover. These processes are included in the COM using the load factor. Theoretical relations are derived in Deltares (2013) for the load factor at geometrical transitions, transitions in cover type and obstacles. The load factor is also calibrated using overtopping tests with the wave overtopping simulator and probability distribution of the load factor for transitions and obstacles are derived in Deltares (2022d).

It is important to realise that the calibration of the load factor based on wave overtopping tests results in significant uncertainty. Firstly, the maintenance of the grass cover around transitions and obstacles is challenging and thereby transitions do not only affect the load, but also the strength of the grass cover. The reduced strength at transitions is included in the COM using the strength factor α_s . Next to the load factor, the critical flow velocity U_c that describes the grass cover strength is also calibrated using the wave overtopping tests. This leads to a dependency between the load factor and critical flow velocity, and therefore multiple combinations of α_m and U_c are possible (Deltares, 2022d).

The theoretical formulas for the load factor derived in Deltares (2013) are summarized in this section for transitions in cover types, slope changes and obstacles. The theoretical values are compared to the calibrated load factors and to recent studies on transitions in the Netherlands (Ponsioen, 2019; Van Bergeijk, 2022a) and the UK (Simm, 2021).

3.3.1 Transitions in cover type

Transitions in cover type affect the flow velocity through the bed roughness. The transition from grass to a smoother cover leads to acceleration of the flow, while the transition from grass to a rough cover results in deceleration of the flow (Van Bergeijk, 2022a). Additionally, the roughness difference can lead to additional turbulence (Deltares, 2013). A theoretical relation for the load factor due to transitions in cover type is given in Deltares (2013). The load decreases for a transition from a rough to a smooth bed leading to the load factor $\alpha_{m,r \rightarrow s}$

$$\alpha_{m,r \rightarrow s} = \left(\frac{n_s}{n_r} \right)^6 \left(\frac{\ln(10h / (8\sqrt{g}n_s)^6)}{\ln(10h / (8\sqrt{g}n_r)^6)} \right)^2 \quad (14)$$

while the load increases for a transition from a smooth to a rough bed

$$\alpha_{m,s \rightarrow r} = 2 - \alpha_{m,r \rightarrow s} \quad (15)$$

With:

n_s : Manning coefficient of the smooth cover (s/m^{1/3}).

n_r : Manning coefficient of the rough cover (s/m^{1/3}).

h : layer thickness (m).

g : gravitational acceleration (m/s²).

These theoretical formulas are based on a study by Nezu and Nakagawa (1993) for currents over smooth and rough bed strips and derived assuming uniform flow conditions. The wave overtopping flow is turbulent and not uniform, so is not clear if these assumptions are valid for the wave overtopping flow.

The theoretical formula (Equation (14)) leads to a load factor of 1.5 – 1.8 for the transition from an asphalt cover (smooth) to a grass cover (rough) (Deltares, 2022d). Calibration of the load factor using the tests with the wave run-up simulator and the wave overtopping simulator lead to a load factor of 1 - 1.8. The wide range is not only the result of the calibration method leading to different combinations of α_m and U_c . Additionally, height difference can occur between the cover types that can lead to an additional load (Section 3.3.3). Deltares (2022d) recommends a wide probability distribution for the load factor between 1.1 – 1.8, where the height difference is an uncertain factor. For transitions in cover type with a small height difference, a smaller load factor is recommended (1.1-1.2) while for transitions with a larger height differences (max 0.1 m) a higher load factor could be used (1.7-1.8).

The analytical formulas of Van Bergeijk (2019) include a friction factor f for the cover type and can be used to calculate the flow velocity along dike profiles with transitions in cover type. The

performance of the analytical formulas for transitions in cover type on the crest and a landward berm is determined by comparing numerical model results of the flow velocity with the analytically calculated flow velocity (Van Bergeijk, 2022a). The analytical formulas predict a similar change in flow velocity as the numerical model and it is concluded that these formulas can accurately calculate the effect of transitions in cover type on the flow velocity. The numerical model results show that transitions in cover type have a limited effect on the overtopping load with a maximum increase of 20% which would translate to $\alpha_m = 1.2$. However, these results only hold for transitions in cover type without a height difference. Van Bergeijk (2022a) showed that transitions in height significantly affect the hydraulic load, which could lead to higher load factors when the cover types are not smoothly connected.

3.3.2 Slope changes

Slope changes occur at the landward crest line and the transition from the landward slope to a horizontal plane at a berm or the toe. In Deltares (2013), formulas for the load factor are derived based on a force balance where the normal force is affected by the centripetal force at the slope change. The change in load due to a change in normal force is captured in the COM by the load factor. For concave transitions, such as the landward toe, the load increases since the centripetal force is downward directed

$$\alpha_m = 1 + \sin\left(\frac{1}{2}\theta\right) \quad (16)$$

For convex transitions such as the landward crest line, the load decreases since the centripetal force is directed upwards

$$\alpha_m = 1 - \sin\left(\frac{1}{2}\theta\right) \quad (17)$$

with θ the difference in slope angle.

For the landward toe, this results in a load factor of 1.23 and 1.12 for a steepness of 1:2 and 1:4, respectively. Validation of the wave overtopping tests results in a load factor of 1.0 – 1.2 which coincides with the theory (Deltares, 2022d). However, calibration of the load factor at the landward toe by Warmink (2020) leads to significant higher load factors of 1.3 – 1.6 for slopes of 1:3 and 1.5-1.8 for slopes of 1:2.3. The differences in calibrated load factors can be related to the calibration method where different acceleration factors are used (graphical method vs constant value of 1.4) and a different criterion for the calibration of the critical flow velocity are used, e.g. first damage or failure (Frankena, 2019; Deltares, 2022d). In the end, a distribution for the load factor at the landward toe between 1 and 1.4 is recommended in Deltares (2022d).

Van Bergeijk et al (2022b) investigated the load at the landward toe using a numerical model. The numerical model shows that the flow velocity is maximal slightly landward of the toe (around 0.5 m behind the toe). A practical formulation for the maximum flow velocity at the landward toe U_{toe} is derived using the numerical model results that combine both the effect of the acceleration along the slope and the slope change

$$U_{toe} = \sqrt{\alpha_m} \alpha_a U_{crest} = \left(0.22 \frac{V \sqrt{L_s}}{\cot(\varphi)^2} + 1.19 \right) U_{crest} \quad (18)$$

with:

- V : the overtopping volume (m^3/m)
- L_s : the length of the landward slope (m)
- $\cot(\varphi)$: the steepness of the landward slope (-)

For a slope length of 15 m and an overtopping volume of 2 m³/m, the load factor calculated with Equation (18) varies between 0.95 for a gentle slope of 1:4 and 1.37 for a steep slope of 1:2 assuming a constant acceleration factor of 1.4. The constant acceleration factor probably overestimates the acceleration of the relatively large volume and gentle slope of 1:4 leading to a load factor that is smaller than 1 for this wave.

Equation (17) predicts a decrease in load at the transition of the landward crest line. However, flow separation at the landward crest line can occur for steep landward slopes and a sharp transition (Ponsioen, 2019; Van Bergeijk, 2022b). This process results in high impact forces at the reattachment location that significantly increase the load leading to high pressures and normal stresses. The conditions for flow separation and impact are not clear yet but this process will only occur for large overtopping volumes and steep landward slopes. The effect of flow separation on the overtopping flow velocity has not been investigated. However, the effect of this process on the flow velocity at the landward toe is included in Equation (18) that is based on model simulations with and without flow separation at the crest line.

3.3.3 Obstacles

Obstacles can affect the overtopping flow in multiple ways such as blockage of the flow, flow concentration and flow separation. The effect of obstacles on the overtopping flow depends on the height, the width, and the orientation of the obstacle (Figure 3.4). In this report, we distinguish three different categories:

- Height transitions perpendicular to the dike. These transitions have relatively small height of the same order as the layer thickness and therefore the amount of overtopping is not significantly limited contrary to high vertical walls or objects.
- Objects perpendicular to the dike such as trees and houses. The waves have to flow around the object and the effect of the object on the flow depends on the width of the object.
- Objects parallel to the dike such as stairs

The effect of obstacles on the overtopping flow and the load factor are described for each category separately.

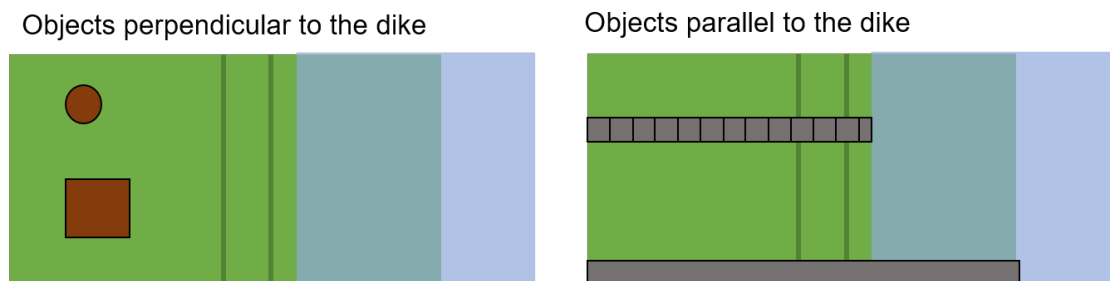


Figure 3.4 Top view of the dike indicating objects perpendicular to the dike, such as trees and houses, and objects parallel to the dike, such as stairs or the transition from a gras-dike to a sluice.

3.3.3.1 Height transitions

Height transitions can lead to flow separation and high impact forces at the reattachment location similar to the wave impact process at the landward crest line (Van Bergeijk, 2022b). The effect of height transitions at an asphalt road is partly incorporated in the load factor for transitions in cover type, where a higher load factor of 1.7-1.8 is recommended for transitions with a height difference (Deltares, 2022d). The increased load due to height transitions have been studied in a numerical model, however, it remains difficult to translate the model results to a load factor in the COM (Van Bergeijk, 2022a). Recent overtopping tests with a height difference

between the grass cover and concrete path indicated that the height difference had no significant effect on the overtopping flow velocity (Deltares, 2021b). Additional research on the effect of height transitions on the flow velocity and the load is required before a load factor for height transitions can be derived.

3.3.3.2 Objects perpendicular to the dike

The additional load due to objects that are located perpendicular to the dike depends on the width / diameter of the object. Wave overtopping test have shown that objects with a width of less than 0.15 m have a limited effect on the overtopping flow and therefore $\alpha_m \approx 1$ (Deltares, 2022d). Based on photos of typical transitions on Dutch dikes, Deltares (2022d) concluded that no grass cover is present around objects that are more than 2 m wide, since these are mainly houses with gardens. Therefore, the COM is not applicable to these cases and no load factor is derived for these wide objects.

For objects between 0.15 and 2 m wide, the overtopping flow will be blocked in front of the object. The flow has to go around the object leading to flow concentration and the flows could meet behind the object leading to an additional load due to mixing. These processes can lead to different loads on the cover in front, to the sides and behind the object. Wave overtopping tests showed no mixing of the flow behind the object, so this process can be neglected for these obstacles (Deltares, 2013). Formulas for the load factor in front and along the object are derived in Deltares (2013) based on expert judgement related to the scour around objects. The load factor in front of the object depends on the drag coefficient C_D that depends on the shape of the object

$$\alpha_m = 1 + \frac{1}{4} C_D \quad (19)$$

The load factor along the object depends on the shape factor K_s

$$\alpha_m = 1.4 K_s \quad (20)$$

An overview of the drag coefficient and shape factors can be found in Appendix B. For trees that have a cylindrical shape, $C_D = 1.2$ and $K_s = 1$ resulting in a load factor $\alpha_m = 1.3$ in front of the tree and $\alpha_m = 1.4$ along the tree (Deltares, 2013). For rectangular shapes such as side wall structures, $C_D = 2$ and $K_s = 1.2$ resulting in a load factor $\alpha_m = 1.5$ in front of the object and $\alpha_m = 1.7$ along the object. A distribution of the load factor between 1-1.8 is recommended in Deltares (2022d) with the highest probability between 1.2-1.5 based on calibration of the overtopping tests and the calculated load factors with Equations (19) and (20).

Pijpers (2013) also calibrated a load factor for objects using the results of the wave overtopping tests. An erosion model based on pressures is used to calibrate the load factor in front of the object, which means that this load factor cannot be used in the COM. However, the COM is used to calibrate the load factor for the flow along the object resulting in a load factor between 1-1.8 depending on the overtopping volume: $\alpha_m \approx 1$ for $V \leq 1500$ l/m, $\alpha_m = 1.4$ for $V = 2500$ l/m and $\alpha_m = 1.8$ for $V = 3000$ l/m. However, it is not completely clear how the acceleration of the landward slope is included in this calibration, but it could be useful to study the effect of the overtopping volume on the load factor. Numerical model simulations in Pijpers (2013) showed that the object had a limited effect on the overtopping flow velocity. This could be an indication that other variables such as the pressure might be better to describe the load on the cover around objects.

3.3.3.3 Objects parallel to the dike

Objects that are located parallel to the dike are also named longitudinal transitions, such as stairs or the transition from a grass-covered dike to another structure. In Deltares (2015), a load factor α_m of 1.0 is calibrated for stairs. However, it is mentioned that good validation of the load factor is not possible using the available overtopping tests and further validation is recommended. Especially in case of wave overtopping as the result of oblique waves, these objects are no longer parallel to the flow direction and therefore the angle of wave-attack could be important for the load factor. It is hypothesized in Deltares (2015) that objects parallel to the flow can lead to additional turbulence, but this could not be observed in the data. Therefore, Deltares (2022d) suggests a load factor of 1-1.3 for objects parallel to the dike.

Numerical model simulations with a CFD model performed by Simm (2021) showed that the flow velocity increases with a factor 1 to 1.34 for objects parallel to the dike and the shear stress can increase to a factor 1.6. The range of this velocity amplification factor is similar to the load factor of 1-1.3 in Deltares (2022d), but again the effect of oblique waves has not been investigated.

3.4 Discussion

The cumulative overload method uses an acceleration factor to describe the acceleration along the landward slope and a load factor to account for transitions and obstacles. Distributions for the load factor are given in Deltares (2022d) and are summarized in this report. This means that the load factor can be used as a stochastic variable in probabilistic computations with the COM as shown in Deltares (2022d). The acceleration factor is currently used by BOI as a deterministic parameter with a value of 1.0 for the crest and 1.4 for the slope. The description of the acceleration factor can be improved using the analytical formulas of Van Bergeijk et al (2019) that are fast and accurate. Another possibility is to make the acceleration factor a stochastic variable and develop a probability distribution for the acceleration factor.

The main advantage of using analytical formulas to describe the flow velocity along the landward slope is to increase the accuracy of the flow velocity by taking the effect of overtopping volume, crest width, slope length, slope steepness and cover type into account. Since the flow velocity is squared in the COM, discrepancies in the flow velocity can blow up. The accuracy of the load can be improved using the analytical formulas of Van Bergeijk et al (2019) that do not need to be solved in an iterative manner and can therefore be cost-effective comparing the computational costs and the increase in accuracy of the flow velocity. Additionally, these formulas can also calculate the effect of transitions in cover type on the overtopping flow velocity, but only for transitions without a height transition.

The analytical formulas result in a lower flow velocity at the end of the crest compared to a constant acceleration factor of 1.0 resulting in a reduction of the load towards the end of the crest. The analytical formulas lead to higher flow velocities at the end of the slope compared to an acceleration factor of 1.4, but this will partly be balanced by a lower flow velocity at the start of the slope. A consequence analysis is necessary to determine what the effect of the analytical formulas on the cumulative load at the landward toe is. Since the parameters in the COM are calibrated, improving the description of the load will require a re-calibration of the thresholds for the damage number, the critical flow velocity, load factor and other parameters in the COM (Deltares, 2015).

Next to the analytical formulas, a formula for the flow velocity at the landward toe is available (Equation (18)) that includes both the deceleration along the crest, the acceleration along the slope and the effect of the slope change at the landward toe. The main benefit of this formula is that only one calculation is necessary to include all these effects. The analytical formulas in combination with the load factor require 4 calculations to obtain the flow velocity at the landward

toe. However, the analytical formulas can also be used to calculate the flow velocity at locations of damages along the slope and Equation (18) is only applicable to the landward slope.

The load factor is used to locally account for the effect of transitions and obstacles. This means that the effect of transitions and obstacles on the downstream flow is not incorporated in the COM. This is contrary to findings that transitions of the overtopping flow affect the downstream flow, both for transitions in cover type as for geometric transitions and obstacles (Van Bergeijk, 2022a). This problem can partly be solved by using a flow velocity along the crest and the landward slope while it is not yet known how to include the effect of height differences and obstacles on the downstream flow

The current description of the load in the COM is based on shear loading described by the flow velocity squared. However, studies have indicated that normal stresses and pressures might be better variables to describe the load due to slope changes, height differences and obstacles (Pijpers, 2013; Ponsioen et al, 2019; Van Bergeijk, 2022a).

The load factor for transitions and obstacles is uncertain resulting in broad distributions for the load factor (Deltares, 2022d). Due to limited data and failure due to secondary effects (Van Steeg et al., 2015), it remains challenging to calibrate the load factor on overtopping tests where even the calibration of the landward toe that has been frequently tested leads to a significant spread in possible load factors. Firstly, the majority of the failures at transitions occur due to secondary effects like maintenance and construction issues. Secondly, both the critical flow velocity and the load factor are calibrated using the same data. The development of an independent method to determine the critical flow velocity, such as grass pulling tests or the fire-hose method, could lead to reduction of the uncertainty in the load factor when this is the only parameter calibrated on the observed damage during overtopping tests.

4 Conclusions and recommendations

4.1 Conclusions

4.1.1 Conclusions – influence factors wave run-up

Often, the basis for the currently used influence factors on run-up is the work of WL|Delft Hydraulics (1993). As a starting point, it is strived to find relations for the different influence factors that are based on an average of experimental research. However, when little data is available, conservative decisions were made.

- The influence factors for roughness are mostly based on conservative assumptions made in TR23A (2002).
- The equations for the influence of oblique waves is based on an average from several tests described in WL|Delft Hydraulics (1993), but the facility (Vinjé facility in Marknesse) is no longer considered as a state-of-the-art facility. This may have influenced the results.
- For the set of equations for the berm influence, most of the equations are based on an average from several tests described in WL|Delft Hydraulics (1993), although a large spread is found in the results. The equations for the height of the berm however have been changed in TAW (2002). It is unclear why these equations are adapted. The validity of the expressions to account for the berm are unknown and indications exist that for some conditions the results are systematically conservative while for other conditions the results are systematically non-conservative.

4.1.2 Conclusions – the overtopping flow velocities

The COM includes two influence factors for the load. The acceleration factor describes the change in flow velocity along the crest and the landward slope. The load factor is used to account for an additional load due to transitions and obstacles.

- Two methods for the acceleration factor are used: a constant acceleration factor of 1.4 for the acceleration along the slope and a graphical method to determine the acceleration factor depending on the slope steepness, slope length and flow velocity on the crest. Although a constant acceleration factor is easy to use, the slope steepness and flow velocity on the crest have a significant influence on the acceleration. Applying a constant acceleration factor is physically not correct, has shown not to match with data, and introduces unnecessary inaccuracies.
- Analytical formulas have been developed to calculate the flow velocity along the crest and the landward slope. These formulas are accurate and practical to use since they do not need to be solved in an iterative manner as is the case for some of the existing formulas. The analytical formulas can improve the description of the flow velocity along the crest and the landward slope by taking the overtopping volume, crest width, slope length, slope steepness and cover type into account. These formulas result in a lower flow velocity at the end of the crest and more acceleration along the slope.
- Distributions for the load factor are derived in Deltares (2022d) for transitions in cover types, slope changes at a berm/toe and for obstacles perpendicular and parallel to the dike. These distributions are based on theoretical formulas and calibration of wave overtopping tests, and the distributions agree with recent studies on transitions. The distributions for the load factors are wide due to the significant uncertainty in the load factor. This is because both the critical velocity and load factor are calibrated on the same data set resulting in multiple combinations that are possible.

4.2 Recommendations

This report has shown that accurately determining influence and acceleration factors has a significant effect on both the wave run-up heights and flow velocities, which are instrumental to the initial mechanisms GEKB and GEBU and a number of subsequent failure mechanisms. It is recommended to analyse whether this significantly improved accuracy in run-up heights and flow velocities also significantly impacts the probability of flooding within the dike safety assessment.

4.2.1 Recommendations – influence factors wave run-up

It is recommended to assess the accuracy of influence factors on wave run-up for smooth dikes (e.g. with grass covers) and to adapt expressions for influence factors to obtain a mean-value estimate of all relevant influence factors and combination of influence factors.

Since the currently used influence factors are mostly based on research from 1993, it is recommended to first add available studies on run-up reduction that have been executed since then. However, recent tests mainly focus on wave overtopping, so the amount of available data is limited. After all available data has been added, new experimental research is needed. Tests for the influence of oblique waves on wave run-up is deemed to be a first step that requires the least number of tests to derive a new formula. New experiments fulfil both the purpose of validating some older data (for instance the tests from the Vinjé facility), as giving a better basis to base the influence factors on average values.

Above approach aims at determining and improving the accuracy of wave run-up prediction in order to assess the velocities that determine the loading on (e.g. grass covered) dikes. Applying existing expressions in the mean-value approach as adopted in BOI leads to an unknown accuracy of the outcome of the evaluation of grass covers at the seaward side of dikes. It is recommended to adopt a probabilistic method to assess the performance of grass covers at the seaward side of dikes based on expressions with a known accuracy.

4.2.2 Recommendations – the overtopping flow velocities

- Firstly, the graphical method is recommended to determine the acceleration factor instead of using a constant value of 1.4. Especially the slope steepness has a significant increase on the acceleration and should be considered in the COM.
- Formulas for the flow velocity along the crest and the landward slope are available (Table 3.2) as well as a practical formula for the flow velocity at the landward toe (Equation (18)). It is recommended to study the use of the formulas proposed by Van Bergeijk et al (2019) for the COM in a consequence analysis to determine how the use of these more accurate formulas than those currently being used affect the COM results before these formulas are implemented. Changing the description of the load in the COM requires recalibration of the COM since both the thresholds for the damage number and the critical velocities are calibrated using the graphical method for the acceleration factor.
- A new method for calibration of the load factor is recommended since the current method where both the load factor and the critical velocity are calibrated using the same dataset results in multiple possible combinations for the load factor and the critical velocity. This can lead to a better estimation of the load factor and presumably will reduce the uncertainty in the load factor and thereby narrow the probability distributions of the load factor for transitions and obstacles.
- Recent studies show that transitions and obstacles result in high normal loads such as normal stresses, normal forces and pressures. These studies provide insight into the processes at transitions and obstacles, but these results cannot yet be translated to a load factor. A different method than the COM is necessary to describe these types of loads. Therefore, it is recommended to study in which cases these normal loads are

important and how to include these loads in the design and safety assessment guidelines.

- It is recommended to study the influence factors that are determined for wave overtopping discharges (for instance for berms and oblique waves), but have not been validated for velocities at the crest and landward slope.

References

- Bosman, G., 2007. Velocity and flow depth variations during wave overtopping. Master thesis, Technical University of Delft, The Netherlands
- Capel, A., 2015. Wave run-up and overtopping reduction by block revetments with enhanced roughness. Coastal Engineering. 104. <https://doi.org/10.1016/j.coastaleng.2015.06.007>.
- Chen, W., Van Gent, M.R.A., Warmink, J.J. & Hulscher, S.J.M.H., 2020. The influence of a berm and roughness on the wave overtopping at dikes. Coastal Engineering. 156. <https://doi.org/10.1016/j.coastaleng.2019.103613>.
- Chen, W., Warmink, J.J., van Gent, M.R.A. & Hulscher, S.J.M.H., 2022. Numerical investigation of the effects of roughness, a berm and oblique waves on wave overtopping processes at dikes. Applied Ocean Research, 118, 1-19, 102971. <https://doi.org/10.1016/j.apor.2021.102971>
- Deltares, 2013. Evaluation and Model Development: Grass Erosion Test at the Rhine dike. Deltares report 1207811-002-HYE-0007-svb, Authors: A. van Hoven, G. Verheij, G. Hoffmans and J. van der Meer.
- Deltares, 2014. Residual strength of grass on river dikes under wave attack. Phase 3: Large scale flume model tests on soil and grass of locations Harculo and Oosterbierum. Deltares report 1207811-009-HYE-0011, Authors: P. van Steeg.
- Deltares, 2015. WTI Onderzoek en ontwikkeling landelijk toetsinstrumentarium, Product 5.12 Analyses grass erosion in wave run-up and wave overtopping conditions. Deltares report 1209437-005-HYE-0003, Authors: J. van der Meer, G. Hoffmans and A. van Hoven.
- Deltares, 2017. Onderbouwing kansverdelingen kritisch overslagdebiet ten behoeve van het OI2014v4 (in Dutch). Deltares report 1230090-011-GEO-0006-jvm Authors: A. van Hoven and J.M. van der Meer.
- Deltares, 2019. BOI Omgaan met overgangen bij faalmechanisme gras erosie kruin en binnentalud, Korte studie naar kansverdelingen van het kritisch overslagdebiet inclusief overgangen (in Dutch). Deltares report 11203720-025-GEO-0001, Authors: A. van Hoven and M. Boers.
- Deltares, 2021a. Harmonisatie van de cumulatieve overbelastingmethode op buiten- en binnentalud (in Dutch). Deltares report 11206817-020-GEO-0001. Authors: P. van Steeg and J.P. den Bieman.
- Deltares, 2021b. Wave run-up velocities for the cumulative overload method for erosion of grass revetments. Deltares report 11206817-034-GEO-0001. Authors: J.P. den Bieman and P. van Steeg.
- Deltares, 2021c. Analyse golfklapproeven en golfoverslagproeven Gras op zand onderzoek product 8 (in Dutch). Deltares report 1204369-002-GEO-0015. Authors: A. van Hoven
- Deltares, 2022a. Wave run-up velocities – derivation of an expression to be used in the cumulative overload method. Deltares report 11208057-037-GEO-0002. Authors: J.P. den Bieman and M.W. Doeleman. (draft)
- Deltares, 2022b. Consequentieanalyse van een nieuwe uitdrukking voor stroomsnelheden in de cumulatieve overbelastingmethode – voor de initiële mechanismen GEKB en GEBU olopzone (in Dutch). Deltares report 11208057-037-GEO-0005. Authors: A.J. Smale and J.P. den Bieman. (draft)

- Deltares, 2022c. Influence of water depth on the wave height, wave run-up and front velocities. Deltares report 11208034-011-ZWS-0001. Authors: M.W. Doeleman and J.P. den Bieman. (draft)
- Deltares, 2022d. Kennis voor keringen GEKB Overgangen en objecten (in Dutch). Deltares report 11206817-021-GEO-0001, Authors: A. van Hoven.
- Deltares, RWS-WVL & HWBP, 2022. Rode draad overstrooming door dijkerosie (in Dutch). (draft)
- EurOtop, 2007. Wave Overtopping of Sea Defences and Related Structures: Assessment Manual. Authors: T. Pullen, N.W.H. Allsop, T. Bruce, A. Kortenhuis, H. Schüttrumpf and J.W. van der Meer.
- EurOtop, 2018. Manual on wave overtopping of sea defences and related structures. An overtopping manual largely based on European research, but for worldwide application. www.overtopping-manual.com
Authors: Van der Meer, J.W., Allsop, N.W.H., Bruce, T., De Rouck, J., Kortenhuis, A., Pullen, T., Schüttrumpf, H., Troch, P. and Zanuttigh, B.
- Formentin, S. M., Gaeta, M. G., Palma, G., Zanuttigh, B., & Guerrero, M., 2019. Flow depths and velocities across a smooth dike crest. *Water*, 11(10), 2197. <https://doi.org/10.3390/w11102197>
- Frankena, M., 2019. Modelling the influence of transitions in dikes on grass cover erosion by wave overtopping. Master thesis, University of Twente, The Netherlands.
- Hoffmans, G.J.C.M. and Verheij H.J., 1997. Scour Manual, Balkema, Rotterdam, The Netherlands
- Hughes, S.A., 2011. Adaptation of the levee erosional equivalence method for the hurricane storm damage risk reduction system (HSDRRS). U.S. Army Engineer Research and Development Center - Coastal and Hydraulics Laboratory, Vicksburg, Missipi, US
- Nezu, I., & Nakagawa, H., 1993. *Turbulence in open-channel flows*. ISBN 9054101180
- Pijpers, R., 2013. Vulnerability of structural transitions in flood defences: erosion of grass covers due to wave overtopping. Master Thesis, Technical University of Delft, The Netherlands.
- Ponsioen, L., van Damme, M., Hofland, B., & Peeters, P., 2019. Relating grass failure on the landside slope to wave overtopping induced excess normal stresses. *Coastal Engineering*, 148, 49-56. <https://doi.org/10.1016/j.coastaleng.2018.12.009>
- SBW, 2012. Wave Overtopping and Grass Cover Strength. Model development. Deltares Report. 120616-007, Authors: G.J. Steendam, G. Hoffmans, J. Bakker, J. van der Meer, J. Frissel, M. Paulissen and H. Verheij
- Schüttrumpf, H., 2001. *Wellenüberlaufströmung an Seedeichen: experimentelle und theoretische Untersuchungen*. PhD Thesis, Braunschweig Technical University, Germany.
- Schüttrumpf, H., & Oumeraci, H., 2005. Layer thicknesses and velocities of wave overtopping flow at seadikes. *Coastal Engineering*, 52(6), 473-495. <https://doi.org/10.1016/j.coastaleng.2005.02.002>
- Simm, J., Woods Ballard, B., Flikweert, J. J., Maren, E. V., Dimakopoulos, A., Hassan, M., ... & Steeg, P. V. , 2021. Investigation, assessment and remediation of levee transitions. In *FLOODrisk 2020-4th European Conference on Flood Risk Management*. Budapest University of Technology and Economics. DOI 10.3311/FloodRisk2020.14.6
- TAW, 1997. Technical Report – Erosion Resistance of grassland as dike covering. *Technical Advisory Committee for Flood Defence in the Netherlands (TAW)*. Delft, The Netherlands. Authors: H.J. Verheij, G.A.M. Kruse, J.H. Niemeijer, J.T.C.M. Sprangers, J.T. de Smidt and P.J.M. Wondergem.

- TAW, 2002. Technisch Rapport golfploop en golfoverslag bij Dijken (in Dutch). Technische Adviescommissie voor de waterkeringen. Delft, The Netherlands.
- TR23A, 2002. Invloedsfactoren voor de ruwheid van toplagen bij golfploop en overslag. Bijlage bij het Technisch Rapport Golfploop en Golfoverslag bij dijken (in Dutch). Report DWW-2002-112. Author: J.W. van der Meer
- van Bergeijk, V. M., Warmink, J.J., van Gent, M.R.A., & Hulscher, S. J.M.H., 2019. An analytical model of wave overtopping flow velocities on dike crests and landward slopes. *Coastal engineering*, 149, 28-38. <https://doi.org/10.1016/j.coastaleng.2019.03.001>
- Van Bergeijk, V.M., 2022a. Over the Dike top: Modelling the Hydraulic Load of Overtopping Waves including Transitions for Dike Cover Erosion. PhD Thesis, University of Twente, The Netherlands. ISBN: 978-90-365-5341-4, DOI 10.3990/1.9789036553414
- Van Bergeijk, V.M., Warmink, J.J., & Hulscher, S.J.M.H., 2022b. The wave overtopping load on landward slopes of grass-covered flood defences: Deriving practical formulations using a numerical model. *Coastal Engineering*, 171, 104047. <https://doi.org/10.1016/j.coastaleng.2021.104047>
- Van der Meer, J.W. & De Waal, J.P., 1990. TAW projectgroep A1: Belastingen – Invloed van scheve inval en richtingspreiding op golfploop en overslag. Report: H638.
- Van der Meer, J. W., Hardeman, B., Steendam, G. J., Schüttrumpf, H., & Verheij, H., 2010. Flow depths and velocities at crest and landward slope of a dike, in theory and with the wave overtopping simulator. *Coastal Engineering Proceedings*, 1(32), 10.
- Van Gent, M.R.A., 2020. Influence of oblique wave attack on wave overtopping at smooth and rough dikes with a berm. *Coastal Engineering* 160, 103734. <https://doi.org/10.1016/j.coastaleng.2020.103734>
- Van Gent, M. R. A., 2002. Low-exceedance wave overtopping events: Measurements of velocities and the thickness of water-layers on the crest and inner slope of dikes. *Delft Hydraulics*, DC1-322-3.
- Van Gent, M. R. A. & van der Werf, I. M., 2019. Influence of oblique wave attack on wave overtopping and forces on rubble mound breakwater crest walls. *Coastal Engineering*, 151 (2019), 78–96. <https://doi.org/10.1016/j.coastaleng.2019.04.001>
- Van Steeg, P., Labruijere, A., & Mom, R., 2015. Transition structures in grass covered slopes of primary flood defences tested with the wave impact generator. *Proceedings of 36th IAHR world congress*. The Hague, The Netherlands, 28 June – 3 July, 2015
- Van Steeg, P., Klein Breteler, M. & Provoost, Y., 2016. Large-scale physical model tests to determine influence factor of roughness for wave run-up of channel shaped block revetments. *Proceedings of Coastlab16*, Canada, May 10-13, 2016
- Van Steeg, P., de Ridder, M.P., Capel, A., Bottema, M., 2020. Influence of water depth on wave overtopping. *Proceedings of 4th European Conference on Flood Risk Management*. Virtual conference, 22 June – 24 June 2022
- Warmink, J.J., van Bergeijk, V.M., Frankena, M., Van Steeg, P., & Hulscher, S.J.M.H., 2020. Quantifying the influence of transitions on grass cover erosion by overtopping waves. *Coastal Engineering Proceedings*, (36v), 39-39. <https://doi.org/10.9753/icce.v36v.papers.39>
- WL|Delft Hydraulics, 1993. Waterbeweging op taluds. Invloed van berm, ruwheid, ondiep voorland en scheve lang- en kortkammige golfaanval (in Dutch). Authors: J.W. van der Meer and J.P. de Waal

WL|Delft Hydraulics, 1997. Golfploop en golfoverslag bij dijken, Projectverslag: achtergronden bij aanpassing van notitie “golfploop en golfoverslag bij dijken” (in Dutch). Report H 2458/ H 305. Authors: J.W. van der Meer.

A Roughness factors TAW

Code	Omschrijving	Invloedsfactor	Vergelijkingsmateriaal
1	Asfaltbeton	1,0	Referentietype
2	Mastiek	1,0	Asfalt
3	Dicht steenasfalt	1,0	Referentietype
4	Open geprefabriceerde steenasfaltmatten	0,9	Geen foto/Fixtone
5	Open steenasfalt	0,9	Referentietype/Fixtone
6	Zandasfalt (tijdelijk of in onderlaag)	1,0	Referentietype
7	Breksteen, gepenetreerd met asfalt (vol en zat)	0,8	Breksteen/asfalt/Vilvoordse steen
8	Baksteen/betonsteen, gepenetreerd met asfalt (vol en zat)	1,0	Ondoorlatend en vrijwel glad
9	Breksteen, gepenetreerd met asfalt (patroonpenetratie)	0,7	Breksteen/asfalt; enkele laag 0,8
10	Betonblokken met afgeschuinde hoeken of gaten ein	0,9	Armorflex
11	Betonblokken zonder openingen	1,0	Referentietype
11.1	Haringmanblokken	0,9	Referentietype
11.2	Diaboolblokken	0,8	1/4 blokken omhoog, maar hoger, dus ruwer
12	Open blokkenmatten, afgestrooid met granulair materiaal	0,9	Armorflex
13	Blokkenmatten zonder openingen in de blokken	0,95	Dichte betonblokken
14	Betonplaten van cementbeton of gesloten colloidaal beton, (in situ gestort)	1,0	Dichte betonblokken
15	Colloidaal beton, (open structuur)	1,0	Asfalt, weinig doorlatend
16	Betonplaten, (prefab)	1,0	Dichte betonblokken
17	Doorgroeiende, beton	0,95	Steen zelf enige ruwheid, maar gras maakt het gladder
18	Breksteen, gepenetreerd met cementbeton of colloidaal beton, (vol en zat)	0,8	Breksteen/asfalt/Vilvoordse steen
19	Breksteen, met patroonpenetratie van cementbeton of colloidaal beton	0,7	Breksteen/asfalt; enkele laag 0,8
20	Gras, gezaaid	1,0	Referentietype
21	Gras, zoden of gezaaid, in kunststofmatten	1,0	Gras
22	Bestorting van grof grind en andere granulaire materialen	0,8	Kleiner dan breksteen, minder ruw. Voorwaarde: stabiel
23	Grove granulaire materialen c.q. breksteen verpakt in metaalgaas	0,7	Kleiner dan breksteen, wel doorlatend
24	Fijne granulaire materialen c.q. zand/grind verpakt in geotextiel, zandzakken	0,9	Enige doorlatendheid en ruwheid
25	Breksteen, (stortsteen)	0,55	Referentietype. Enkele laag 0,7
26	Basalt, gezet	0,9	Referentietype
26.01	Basalt, gezet, ingegoten met gietasfalt	0,95	Basalt, zonder doorlatendheid
26.02	Basalt, gezet, ingegoten met colloidaal beton of cementbeton	0,95	Basalt, zonder doorlatendheid
27	Betonzuilen en andere niet rechthoekige blokken		
27.1	Basalton	0,9	Basalt
27.2	PIT Polygoon zuilen	0,9	Basalt
27.3	Hydroblock	0,9	Basalt; Ecoblock 0,9
27.01	Betonzuilen of niet rechthoekige blokken, ingegoten met gietasfalt	1,0	Asfalt, vrijwel glad en ondoorlatend
27.11	Basalton, ingegoten met gietasfalt	1,0	Asfalt, vrijwel glad en ondoorlatend
27.21	PIT Polygoon zuilen, ingegoten met gietasfalt	1,0	Asfalt, vrijwel glad en ondoorlatend
27.31	Hydroblock, ingegoten met gietasfalt	1,0	Asfalt, vrijwel glad en ondoorlatend
27.02	Betonzuilen of niet rechthoekige blokken, ingegoten met beton	1,0	Asfalt, vrijwel glad en ondoorlatend
27.12	Basalton, ingegoten met beton	1,0	Asfalt, vrijwel glad en ondoorlatend
28	Natuursteen, gezet		
28.1	Vilvoordse	0,85	Referentietype
28.2	Lessinische	0,85	Vilvoordse
28.3	Doomikse	0,9	Basalt
28.4	Petit graniet	0,90	Basalt
28.5	Graniet	0,95	Basalt, iets minder open
28.6	Noordse of Drentse steen	0,75	Enkele laag breksteen, iets minder doorlatend
28.01	Natuursteen, gezet, en ingegoten met gietasfalt		
28.11	Vilvoordse, ingegoten met gietasfalt	0,95	Asfalt, vrijwel glad en ondoorlatend
28.21	Lessinische, ingegoten met gietasfalt	1,0	Asfalt
28.31	Doomikse, ingegoten met gietasfalt	1,0	Asfalt
28.41	Petit graniet, ingegoten met gietasfalt	1,0	Asfalt
28.51	Graniet, ingegoten met gietasfalt	1,0	Asfalt
28.61	Noordse of Drentse steen, ingegoten met gietasfalt	0,85	Enkele laag breksteen, veel minder doorlatend
28.02	Natuursteen, gezet, en ingegoten met beton		
28.12	Vilvoordse, ingegoten met beton	0,95	Asfalt, vrijwel glad en ondoorlatend
28.22	Lessinische, ingegoten met beton	1,0	Asfalt
28.32	Doomikse, ingegoten met beton	1,0	Asfalt
28.42	Petit graniet, ingegoten met beton	1,0	Asfalt
28.52	Graniet, ingegoten met beton	1,0	Asfalt
28.62	Noordse of Drentse steen, ingegoten met beton	0,85	Enkele laag breksteen, veel minder doorlatend
29	Koperslabblokken	1,0	Dichte betonblokken
30	Klei onder zand		niet van toepassing
31	Bestorting van natuursteenmassa	0,55	Dubbele laag breksteen; bijvoorbeeld kreukelberm
32	Klinkers, beton of gebakken, zand	1,0	Dichte betonblokken, voegen dicht met gras
33	zand		niet van toepassing
34	steenfundering, gebonden		niet van toepassing
36	kade, keermuur, kistdam		niet van toepassing

B Drag coefficients and shape parameters for objects

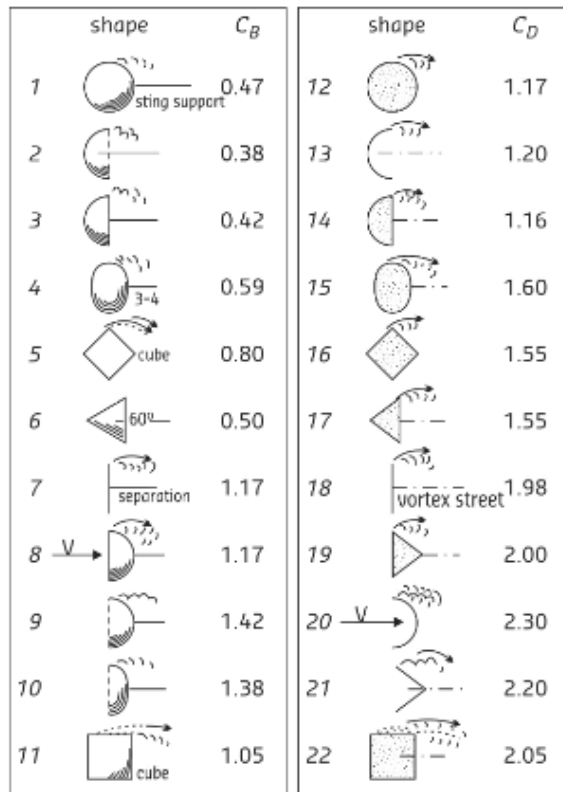


Figure B.1 The drag coefficients for 2D (right side) and 3D (left side) objects for Reynolds numbers between 10^4 to 10^5 as described in Deltares (2013).

Table B.1 The shape factor for different obstacles (Deltares, 2013; Hoffmans and Verheij, 1997).

Form of the cross section	K_s	
Horizontal	Lenticular	0.7-0.8
	Elliptic	0.6-0.8
	Circular	1.0
	Rectangular	1.0 - 1.2
	Rectangular with semi-circular nose	0.9
	Rectangular with chamfered corners	1.01
	Rectangular nose with wedge-shaped tail	0.86
	Rectangular with sharp nose 1:2 to 1:4	0.65 - 0.76
Vertical	Pyramid-like (narrowing upwards)	0.76
	Inverted pyramid (broadening upwards)	1.2

Deltares is an independent institute for applied research in the field of water and subsurface. Throughout the world, we work on smart solutions for people, environment and society.

Deltares

www.deltares.nl